JSCDM

JOURNAL OF SOFT COMPUTING AND DATA MINING
e-ISSN: 2716-621X

Vol. 7 No. 2 (2026) 295-329
https://publisher.uthm.edu.my/ojs/index.php/jscdm

Energy-Based Multi-Objective Black Hole Optimization with Angle Quantization and Crowding Distance for Multi-Objective Optimization Problems

Zeyad Ibrahim Bakri[1,2]*, Salman Yussof[3], Nur Fadilah Ab Aziz[4], Mustafa Musa Jaber[5,6]

1 *Department of Electrical and Electronics Engineering, College of Engineering, Universiti Tenaga Nasional, Kajang, Selangor 43000, MALAYSIA*
2 *Scientific Research Commission, Baghdad, 10070, IRAQ*
3 *Institute of Informatics and Computing in Energy, Universiti Tenaga Nasional, Kajang, Selangor 43000, MALAYSIA*
4 *Institute of Power Engineering, Universiti Tenaga Nasional, Kajang, Selangor 43000, MALAYSIA*
5 *Department of Cybersecurity, Al Hikma University College, Baghdad, IRAQ*
6 *Center of Research and Innovation Management, Universiti Teknikal Malaysia, Melaka, MALAYSIA*

*Corresponding author: engziyed@gmail.com
DOI: https://doi.org/10.30880/jscdm.2026.07.02.017

Article Info

Received: 10 October 2025
Accepted: 20 April 2026
Available online: 30 June 2026

Keywords

Multi-objective optimization, black hole optimization, energy-based algorithms, physics-inspired metaheuristics, adaptive mechanisms

Abstract

Multi-objective optimization (MOO) is a technique that deals with many conflicting goals that seek Pareto-optimal trade-off solutions. Although well-known Multi-Objective Evolutionary Algorithms (MOEAs), including NSGA-II, NSGA-III, MOPSO, and MOEA/D, are still actively used, issues of adaptive exploration-exploitation ratio and distribution control continue to be observed in some problem landscapes. The proposed algorithm EMOBHO-AQCD, is a physics-based bi-objective optimization model that combines three coordinated mechanisms to achieve adaptive search regulation (1), directional diversity control (2), and local density preservation (3). The algorithm represents optimization as a gravitational interaction system whereby elite solutions actively dynamically control search pressure depending on improvement-based energy updates. The suggested approach is compared to four established algorithms (NSGA-II, NSGA-III, MOPSO, and MOEA/D) and three proposed variants (MOBHO, EMOBHO, and EMOBHO-AQCD) on six classical bi-objective benchmark problems based on several performance indicators and non-parametric statistical confirmation (Wilcoxon signed-rank test with Cohen's d effect size analysis at α = 0.05). Findings show that EMOBHO-AQCD is always improving on its predecessors (EMOBHO and MOBHO) and is equally efficient as the major algorithms like NSGA-II and MOPSO in a number of benchmarks. Dominance robustness on low-to-moderate dimensional problems is confirmed by strong set coverage (SC1 = 0.83-1.00), whereas diversity metrics indicate a specified convergence-distribution trade-off profile. Higher-dimensional problems of ZDT are known to be of performance limitation, thus explaining the scope of operations of the proposed framework. In general, EMOBHO-AQCD offers a competitive and bi-objective optimization method, which has specific advantages in stability of dominance and directional coverage, and has a clear and transparent scaling limits in the studied benchmark domain.

1. Introduction

Multi-objective optimization (MOO) is a fundamental approach for finding solutions to engineering and scientific problems with multiple conflicting goals to be optimized at the same time [1, 2]. In comparison with single-objective optimization that tries to obtain a single optimal solution, MOO tries to provide an approximation of a set of Pareto-optimal solutions of trade-offs among competing criteria [1]. These trade-offs are vital in applications, such as in engineering design, logistics, environmental management, and optimization of control systems, where an aspect of performance is bound to be in the trade-off with another [3, 4] . Multi-Objective Evolutionary Algorithms (MOEAs) have been widespread methods of approximating Pareto fronts over the last several decades, in search spaces of complexity [5].

Algorithms like NSGA-II [1], NSGA-III [6], MOEA/D [7], and MOPSO [8] These are representative algorithms that have been shown to perform well on both benchmark and practical optimization problems. Although effective, a number of long-standing challenges persist, such as ensuring a stable ratio between exploration and exploitation, a balanced distribution along irregular or disconnected Pareto fronts, and effective selection pressure across the various stages of optimization [9, 10]. The challenges are especially applicable in engineering when optimizing the controller in renewable energy systems, where optimization landscapes can be multimodal, and Pareto structures can be complicated [11].

Other metaheuristic models that form physics-inspired optimization algorithms represent interactions between solutions as natural laws, such as gravity and thermodynamics [12, 13]. The Black Hole Optimization (BHO) algorithm is one of them and is the closest replica of gravitational attraction, in which the optimal candidate solution is treated as a black hole that pulls other solutions (stars) into its event horizon [14, 15]. Due to its simple and yet effective attraction mechanism, BHO has shown promising behavior in single-objective optimization [16].

Multi-objective extensions, including MOBHO, also use non-dominated sorting and crowding-distance to approximate Pareto fronts [17]. Nevertheless, the current variants of the multi-objective black hole have structural constraints. Lifecycle management of elite solutions generally does not explicitly adapt to improvement dynamics during optimization [18]. In most cases, the preservation of diversity depends on one density-based mechanism and can cause uneven distribution of solutions in irregular Pareto geometries [19, 20]. In order to overcome the constraints, EMOBHO-AQCD implements three coordinated mechanisms, namely: (1) improvement-based energy lifecycle management that enables adaptive selection pressure via dynamic control of elite influence; (2) angle quantization-based sector control [21], to enhance balanced coverage over the objective space; (3) crowding-distance archive management, which guarantees local density control as well as distribution quality in the non-dominated archive [1].

The suggested approach is concerned with the bi-objective problems of optimization, where convergence strength and distribution homogeneity are both prioritized. The performance is to be tested on six benchmark problems, which are classical with two objectives, and compared with that of NSGA-II [1], NSGA-III [6], MOPSO [22], MOEA/D [7], and MOBHO [17] by using several complementary performance measures and statistical validation processes [10].

The main contributions of this work are as follows:

- Integrated Adaptive Framework: Adaptive extension of MOBHO that features improvement-driven energy lifecycle regulation with directional (angle quantization) and density-based (crowding distance) diversity control in a unified gravitational model.
- Structured Benchmarking: Comparative analysis on six classical bi-objective benchmark problems in terms of five state of the art algorithms based on eight convergence and diversity performance measures.
- Robust Statistical Validation: Usage of paired t-tests across all compared algorithms and non-parametric Wilcoxon signed-rank tests, effect-size analysis (Cohen's d), and 95% confidence interval estimation over 20 independent runs at $\alpha = 0.05$ significance level to enhance the credibility of comparison inferences.
- Performance Characterization: Systematic determination of the strengths and weaknesses of the tested bi-objective benchmark scope, which can be used to guide the application in the right context.

The rest of this paper is structured in the following way: Section 2 is a literature review in multi-objective optimization. In Section 3, the EMOBHO-AQCD methodology is discussed. Section 4 is the experimental design and benchmark problems. Section 5 presents the results. Section 6 provides further discussion of findings. The final Section 7 comprises the conclusion and future research directions.

2. Related Studies

This section reviews relevant literature in three areas: (A) relevant benchmark multi-objective optimization algorithms, (B) development of physics-inspired optimization algorithms, and (C) research gaps that led to the development of the proposed EMOBHO-AQCD framework.

2.1 Multi-Objective Optimization Algorithms

Multi-objective optimization algorithms are algorithms that address multiple mathematical problems at once by operating together on multiple objectives with the goal of maximizing their overall utility.
The prevailing paradigm of approximating Pareto-optimal sets of solutions in complex optimization problems is multi-objective evolutionary algorithms (MOEAs) [3] [4]. Of these, NSGA-II [1] It is among the most powerful algorithms, which utilizes rapid non-dominated sorting and crowding distance in achieving a balance between convergence and diversity. Regardless of being robust and widely used, NSGA-II can have an uneven distribution of solutions on irregular or disconnected Pareto fronts [9].

In order to deal with the scalability problem, NSGA-III was proposed as a reference-point-based extension of NSGA-II for many-objective optimization [6]. NSGA-III preserves diversity in higher-dimensional objective spaces by replacing crowding distance with structured reference points. Nevertheless, its performance depends on the configuration and distribution of reference points [6]. Multi-Objective Particle Swarm Optimization (MOPSO) is an extension of particle swarm optimization to a multi-objective setting that includes external archives and leader-selection strategies [22]. Variants of MOPSO rely on density estimation to enhance diversity preservation and convergence efficiency [9]. The other commonly used model is MOEA/D, which breaks a multi-objective problem into several scalar sub-problems that are simultaneously solved using weight vectors [7]. Methods based on decomposition provide computational efficiency and scalability benefits, but can fail in situations where Pareto fronts are very irregular or disconnected [3].

Multi-Objective Black Hole Optimization (MOBHO) is introduced in this paper as an extension of BHO [14] incorporating non-dominated sorting and crowding distance mechanisms [1] to approximate the Pareto front. MOBHO models candidate solutions as stars attracted toward elite black holes according to gravitational principles [15]. Although effective in certain contexts, MOBHO generally uses fixed interaction rules and heavily depends on crowding distance to preserve diversity [18], which may limit its flexibility across different problem landscapes. Such a wide range of algorithms allows thorough comparison of dominance-based (NSGA-II), reference-point-based (NSGA-III), swarm-based (MOPSO), decomposition-based (MOEA/D), and physics-inspired (MOBHO) optimization paradigms. Additionally, most current MOEAs rely on rather fixed interaction dynamics and static population structures during the optimization process, and thus may not be able to dynamically balance exploration and exploitation at different stages of search.

2.2 Evolution of Physics-Inspired Optimization

The metaheuristic algorithms based on physics simulate the processes of optimization with references to natural laws such as gravity, gas solubility, and other physical interactions [12, 13]. The purposes of these approaches are to provide alternative dynamics of search that is not similar to the conventional evolutionary operators. In the Gravitational Search Algorithm (GSA), candidate solutions are represented as masses interacting with each other through the force of gravity [23]. Even though the convergence of GSA was found to be good, it may exhibit a poor performance in high-dimensional spaces, as a result of complex interaction dynamics [24].

In the Black Hole Optimization (BHO) algorithm, gravitational modeling was reduced, where the best solution is regarded as a black hole to attract candidate solutions (stars) into its event horizon [14, 16]. This mechanism has great exploitation potential and has a comparatively low level of computation. An associated multi-objective generalization of BHO, AMOBH [25], uses Shannon entropy and cell density as diversity management tools; it is, however, different from the proposed MOBHO both in terms of its archive implementation and in terms of energy-based lifecycle control and angle quantization. Pareto dominance and crowding-distance archive management [1] were incorporated into MOBHO as a multi-objective baseline extension of BHO [14].

Nevertheless, the current black hole-based multi-objective variants tend to use fixed lifecycle frameworks and static influence mechanisms [15]. In existing black hole-based MOO methods, improvement-driven energy lifecycle regulation has not yet been explicitly implemented, in which elite solutions dynamically adjust their influence based on their measurable contribution to solution improvement [19, 20].

2.3 Research Gaps and Motivation

Based on the reviewed literature, there are still a number of structural limitations in existing multi-objective evolutionary and physics-inspired optimization frameworks. These limitations motivate the proposed improvements in EMOBHO-AQCD.

- Gap 1: Limited Adaptive Exploration–Exploitation Regulation. Most existing MOEAs use fixed control parameters and static interaction rules throughout the optimization process. Although these configurations are stable, they may not adapt to varying optimization phases or landscape characteristics and can lead to premature convergence or inefficient search behavior [9, 18]. Although adaptive variants exist, explicit improvement-driven lifecycle regulation remains relatively underexplored within black hole–based multi-objective frameworks.
- Gap 2: Incomplete Directional Diversity Management. Crowding distance mechanisms and reference-point strategies of diversity preservation are more concerned with density or predefined structural distribution. Nevertheless, such mechanisms do not always guarantee balanced angular coverage of irregular or disconnected Pareto fronts, especially in problems with complex geometries [9, 22]. As a result, clustering or uneven distribution can occur in some regions of the objective space.
- Gap 3: Absence of Performance-Driven Energy Lifecycle Mechanisms in Black Hole MOO Variants. The currently used black hole multi-objective extensions include Pareto dominance and archive management, but they typically apply fixed influence structures for elite solutions [15, 18]. Explicit performance-driven energy regulation in which elite influence is dynamically adjusted according to measurable contribution to solution improvement has not been systematically incorporated in existing black hole multi-objective formulations [6, 19].

Positioning of EMOBHO-AQCD

To address these limitations, the proposed EMOBHO-AQCD framework incorporates:

- Improvement-driven energy lifecycle management, enabling adaptive selection pressure through dynamic regulation of elite influence,
- Angle quantization–based sector control, promoting directional balance across the objective space [21], and
- Crowding-distance archive management, ensuring local density preservation within the non-dominated set [1].

Within the scope of bi-objective optimization problems, this integrated framework extends MOBHO by incorporating adaptive regulation and enhanced diversity control mechanisms.

3. Methodology

The Energy-Based Multi-Objective Black Hole Optimization with Angle Quantization and Crowding Distance (EMOBHO-AQCD) is a physics-inspired multi-objective optimizer, which represents candidate solutions as stars under gravitational-like dynamics influenced by elite black holes. It builds on black hole-based optimization [14, 16] and its multi-objective counterpart MOBHO, but adds an improvement-driven energy lifecycle for elite solutions, as well as directional diversity control through angle quantization [21] and local density control through crowding-distance archive management [1]. In contrast to conventional black hole-based multi-objective variants, where influence/lifecycle rules are typically fixed [18], EMOBHO-AQCD adapts the influence of each black hole based on measurable progress achieved by its associated stars. This brings about self-regulated selection pressure, which supports a stable exploration–exploitation balance while maintaining consistent coverage of the objective space through sector control and preventing archive clustering through crowding distance [1, 21].

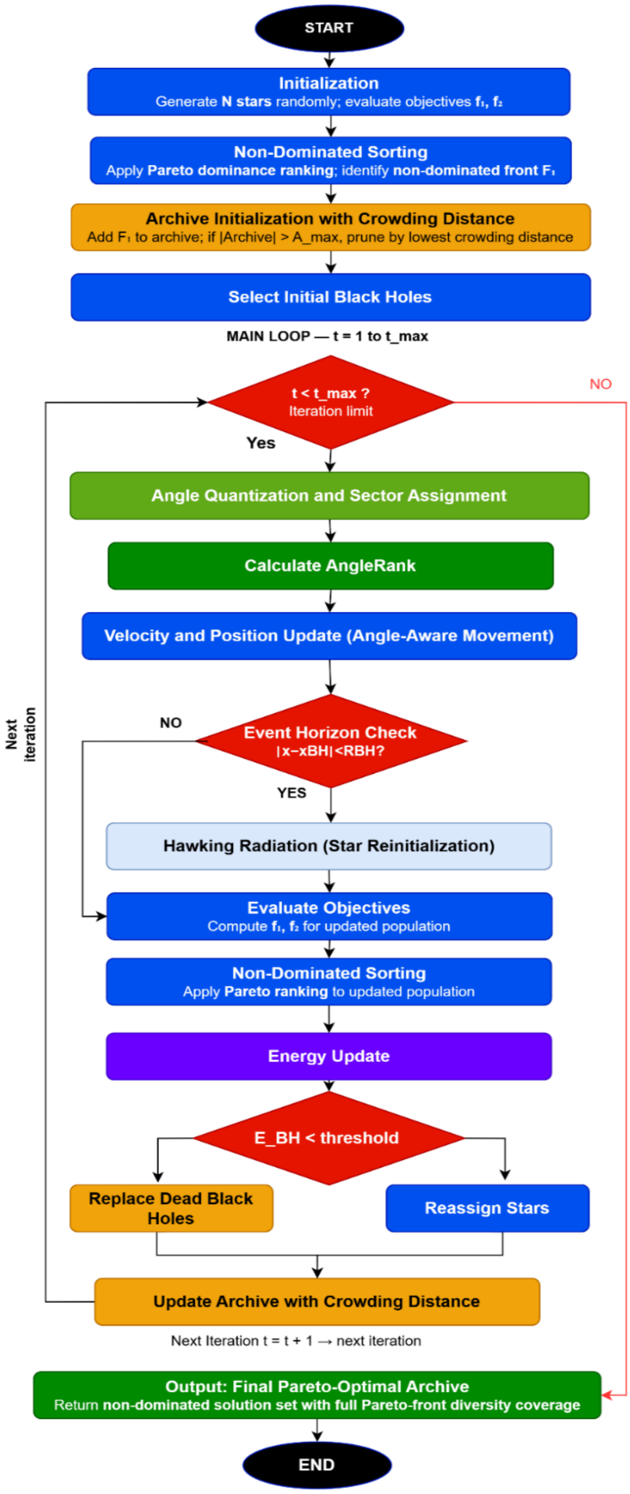

Fig. 1 *Flowchart of the EMOBHO-AQCD framework*

3.1 Problem Formulation

This work addresses bi-objective optimization problems with exactly two objectives:

$$\min \mathbf{f}(\mathbf{x}) = [f_1(\mathbf{x}), f_2(\mathbf{x})]^T \tag{1}$$

subject to:

$$g_j(\mathbf{x}) \leq 0, j = 1, \ldots, J \tag{2}$$

$$h_k(\mathbf{x}) = 0, k = 1, \dots, K \tag{3}$$

$$\mathbf{x} \in \Omega \subseteq \mathbb{R}^n \tag{4}$$

where **x** is the decision vector and Ω is the feasible region. In multi-objective optimization, the solution is a **set** of trade-off solutions (Pareto-optimal set), and their objective values form the **Pareto front**.

Definition 1 (Pareto Dominance): x_1 dominates x_2 (denoted $x_1 \prec x_2$) if:

$$f_i(\mathbf{x}_1) \leq f_i(\mathbf{x}_2), \forall i \tag{5}$$

$$\exists j: f_j(\mathbf{x}_1) < f_j(\mathbf{x}_2) \tag{6}$$

Definition 2 (Pareto Optimality): x∗ is Pareto-optimal if no feasible solution dominates it.

3.2 Core Algorithmic Mechanisms

EMOBHO-AQCD is a combination of three coordinated processes:

- gravitational attraction guided by elite black holes,
- angle quantization for directional balance, and
- crowding-distance archive control for local density preservation [1, 21].

3.3 Algorithmic Components

3.3.1 Gravitational Attraction with Energy-Weighted Influence

The attraction between star i and black hole j is modeled as:

$$A_{ij} = \frac{E_{bh_j}}{\left\| f(x_i) - f\left(x_{bh_j}\right) \right\|^2 + \varepsilon} \tag{7}$$

where:

- A_{ij}: Attraction or influence of black hole j on star i
- E_{bh_j}: Energy of black hole j
- $f(x_i)$: Fitness of star i
- $f\left(x_{bh_j}\right)$: Fitness of black hole j
- ε: A small constant to prevent division by zero

This formulation extends the classical gravitational model by treating energy as a dynamic mass equivalent, enabling a stronger influence from black holes that demonstrate sustained performance improvements.

3.3.2 Angle Quantization Model

The angle quantization mechanism divides the solution space into angular sectors, each having an angle α (the quantization factor). The number of sectors in the solution space is 2π/α. For each solution x_i, the angular direction in objective space is computed as:

$$\theta_i = \operatorname{atan2}\big(f_2(x_i), f_1(x_i)\big) \tag{8}$$

where atan2(·) ensures correct quadrant identification.
The corresponding angular sector index is determined as:

$$\text{Sector}_{\,i} = \left\lceil \frac{\boldsymbol{\theta}_i}{\alpha} \right\rceil \tag{9}$$

where:

- θi is the angular position of solution xi.
- α is the sector width (quantization factor),
- [.] denotes the ceiling function,

J. of Soft Computing and Data Mining Vol. 7 No. 2 (2026) p. 295-329

- Sector $_i$ represents the sector index of solution xi.

To measure directional density, the number of solutions assigned to each sector is calculated as:

$$\text{AngleRank}_s = | \{x_i \colon \text{Sector}_i = s\} | \tag{10}$$

where AngleRank $_s$ denotes the number of solutions in sector s.

This mechanism promotes uniform directional coverage of the Pareto front by encouraging exploration in sparsely populated sectors while reducing clustering in densely populated regions.

3.3.3 Rank-Based Mass Assignment

A mass-like term reflects solution quality using non-dominated rank:

$$M_{\mathrm{i}} = \left(\frac{1}{rank_{\mathrm{i}} + 1}\right) \tag{11}$$

where $rank_{\mathrm{i}}$ denotes the non-dominated sorting rank of solution i.

Solutions with lower ranks (higher quality) obtain larger masses, leading to a stronger influence during movement updates.

3.3.4 Crowding Distance Integration.

To preserve local density, the crowding distance of each solution is computed using the standard NSGA-II formulation [1]:

$$CD_i = \sum_{m=1}^{M} \frac{f_m^{i+1} - f_m^{i-1}}{f_m^{max} - f_m^{min}} \tag{12}$$

where:

- M =2 the number of objectives
- $f_m^{i+1} and\ f_m^{i-1}$ are neighboring objective values in sorted order,
- $f_m^{max} and\ f_m^{min}$ denote the maximum and minimum values of objective m.

To jointly account for local density and directional distribution, a combined diversity metric is defined as:

$$\text{DiversityScore}_i = w_1 \cdot \frac{1}{CD_i + \varepsilon} + w_2 \cdot \frac{1}{\text{AngleRank}_{\text{Sector}_i} + 1} \tag{13}$$

- where w_1 and w_2 are weighting factors ($w_1 = 0.6$, $w_2 = 0.4$).
- AngleRank $_{\text{Sector}_i} + 1$ represents the number of solutions in the same angular sector as solution i,
- ε is a small constant preventing division by zero.

This dual mechanism ensures that solutions in sparse regions, either locally (crowding) or directionally (angular sectors), receive a higher diversity preference.

3.3.5 Velocity/Position Update with Directional Guidance

Each star updates its velocity and position based on inertia, personal best experience, and the force exerted by the assigned black hole:

$$v_i^{k+1} = w \cdot v_i^k + c_1 \cdot r_1 \cdot \frac{M_{\text{pbest}_i}}{M_i} \cdot \left(x_{\text{pbest}_i} - x_i^k\right) + c_2 \cdot r_2 \cdot F_{\text{bh}} \tag{14}$$

where:

- w: Inertia weight (typically 0.9)
- c_1, c_2: Acceleration coefficients (typically 2.0)
- r_1,r_2 ~ U(0,1) are uniformly distributed random numbers,
- M_i is the mass of i,
- F_{bh} Force exerted by the assigned black hole.

The force term incorporates both gravitational attraction and directional diversity control:

$$F_{\mathrm{bh}} = A_{ij} \cdot \frac{x_{\mathrm{bh}_j} - x_i}{\left\| x_{\mathrm{bh}_j} - x_i \right\|} \cdot \frac{1}{\mathrm{AngleRank}_{\,i} + 1} \tag{15}$$

The normalization term ensures that only directional influence is applied, while the factor

$$\frac{1}{\mathrm{AngleRank}_{\,i} + 1}$$

increases the force magnitude for solutions located in sparsely populated angular sectors, thereby promoting uniform directional coverage of the Pareto front.

3.3.6 Event Horizon and Hawking Radiation Mechanism

This formulation ensures that higher-energy black holes generate larger influence regions, enabling adaptive control of exploration intensity.

$$R_{bh_j} = R_{\min} + (R_{\max} - R_{\min}) \cdot \left(\frac{E_{bh_j} - E_{\mathrm{threshold}}}{E_{\max} - E_{\mathrm{threshold}}} \right)^{\beta} \tag{16}$$

where:

- R_{bh_j}: Influence radius of black hole j.
- E_{bh_j}: *Energy of black hole j*,
- E_{max}: Maximum energy among all black holes,
- R_{min}, R_{max} are the minimum and maximum radius factors,
- $\beta > 0$ is the radius scaling exponent (typically $\beta = 1$),
- $E_{threshold}$ is the survival energy threshold,

If the Euclidean distance between star i and black hole j satisfies:

$$||x_i - x_{\beta h}j|| < R_{\beta}hj$$

The star is reinitialized uniformly within the decision space:

$$x_i^{new} = x_{min} + \mathrm{rand}\ (0,1) \cdot (x_{max} - x_{min}) \tag{17}$$

where rand (0,1) denotes a uniformly distributed random vector in [0,1].

The mechanism increases population variety and prevents stagnation by introducing new candidate solutions into the search space at regular intervals. The dynamic radius enables successful black holes to influence broader regions, while weaker black holes maintain smaller spheres of influence.

3.4 Energy Management System

The adaptive core of EMOBHO-AQCD is the energy management mechanism. It enables black holes to dynamically evolve according to their effectiveness in guiding the population toward improved Pareto front approximations. Each black hole is initialized with an equal energy level:

$$Einitial = 100$$

Ensuring unbiased initial influence among elite solutions.

3.4.1 Improvement Calculation

The improvement achieved by star i between consecutive iterations is quantified using hypervolume contribution in the objective space:

$$\Delta_i^k = HV\left(S \cup \{x_i^k\}\right) - HV\left(S \cup \{x_i^{k-1}\}\right) \tag{18}$$

where:

- S denotes the current non-dominated solution set,
- HV $(\cdot)$ represents the hypervolume indicator,

- x_i^k *and* x_i^{k-1} are the positions of star i at iterations k and k−1, respectively.

A positive value of Δ_i^k indicates improvement in Pareto front approximation, while non-positive values indicate stagnation or degradation.

3.4.2 Energy Update

The energy of each black hole is updated using the accumulated improvements of its assigned stars, together with a directional diversity bonus:

$$E_{bh_j}^{k+1} = E_{bh_j}^{k} - \delta_{decay} + \gamma \sum_{i \in S_{bh_j}} \left(\Delta_i^k + \lambda \cdot \frac{1}{\mathrm{AngleRank}_{\ \mathrm{Sector}\ i} + 1} \right) \quad (19)$$

where

- $E_{bh_j}^{k+1}$ is the energy of the black hole j at iteration k,
- δ_{decay} is the energy decay rate,
- γ is the energy gain coefficient,
- S_{bh_j} denotes the set of stars assigned to black hole j
- λ controls the influence of directional diversity,
- $\mathrm{AngleRank}_{\ \mathrm{Sector}\ i}$ represents the density of the angular sector containing star i,

This formulation rewards black holes that generate performance improvements while maintaining stars in sparsely populated sectors, thereby reinforcing both convergence and distribution quality.

3.4.3 Black Hole Replacement

If the energy of a black hole falls below a predefined threshold:

$$E_{bh_j} < E_{\mathrm{threshold}}$$

The black hole is removed and replaced by selecting a new elite solution from the archive according to:

$$P_{\mathrm{selection}\ ,i} \propto \frac{1}{\mathrm{rank}_i + 1} \cdot \ \mathrm{DiversityScore}_{\ i} \quad (20)$$

where:

- rank_i is the non-dominated sorting rank,
- $\mathrm{DiversityScore}_{\ i}$ is defined in Eq. (13).

After replacement, orphaned stars are reassigned to the updated set of black holes to ensure continuity of the search process.

3.5 Complete Algorithm Procedure and Implementation

The entire EMOBHO-AQCD algorithm is summarized in Table 1, with all processes that are defined as initialization, non-dominated sorting, crowding-distance-based archive updating and pruning, angular sector density, velocity, position, event-horizon reinitialization, energy, black hole replacement, and star reassignment. The style of implementation, such as the fast non-dominated sorting and the crowding distance calculation, is the standard procedure of NSGA-II [1].

Table 1 *Pseudocode for EMOBHO-AQCD main framework*

Algorithm 2: EMOBHO-AQCD Main Framework
Data: Population size N, Max iterations T, Archive size A_max, Energy parameters δ_decay, γ, E_threshold, E_initial = 100 Result: Approximated Pareto front PF^A 1 Initialize star population: random positions x_i, velocities v_i 2 Initialize empty archive A; assign E_initial to each black hole 3 Evaluate objective functions f1, f2 for all stars

Algorithm 2: EMOBHO-AQCD Main Framework

```
Perform non-dominated sorting
Calculate crowding distance (see Section 3.3.4)
Update archive A with non-dominated solutions
if |A| > A_max then prune A by the lowest crowding distance
Select n_BH black holes from A probabilistically
for k = 1 to T do
    Compute the angular sector assignment for each solution in A
    Update AngleRank for each star based on sector density
    for each star i do
        Compute gravitational force F_bh from the assigned BH
        Update velocity v_i using pbest and F_bh
        Update position x_i; enforce boundary constraints
        if ||x_i − x_BH_j|| < R_BH_j then
            Reinitialize x_i randomly (Hawking radiation)
        end
    end
    Evaluate objective functions f1, f2 for updated stars
    Perform non-dominated sorting; calculate crowding distance
    Update archive A with new non-dominated solutions
    if |A| > A_max then prune A by the lowest crowding distance
    for each black hole j do
        Sum improvements Δ_i from assigned stars
        Update energy E_BH_j using improvements and AngleRank
        if E_BH_j < E_threshold then mark BH_j for replacement
    end
    Replace dead black holes from A probabilistically
    Reassign orphaned stars to remaining/new black holes
end
return archive A as Pareto front approximation PF^A
```

3.6 Parameter Configuration

Every experiment has a set of fixed parameters to promote fair comparison between benchmark problems. Table 2 contains the EMOBHO-AQCD full configuration.

Table 2 *EMOBHO-AQCD parameter configuration*

Parameter Category	Parameter Name	Symbol	Value
General	Population size	N	100
	Maximum iterations	T	100
	Archive size	A	100
	Number of black holes	N_bh	5
Energy System	Initial energy	E_0	100
	Energy decay rate	δ_decay	10
	Energy threshold	E_threshold	50
	Energy gain factor	γ	5.0
Angle Quantization	Quantization factor	α	$\pi/8$
	Diversity weight 1	w_1	0.6
	Diversity weight 2	w_2	0.4
Gravitational	Inertia weight	w	0.9
	Cognitive coefficient	c_1	2.0
	Social coefficient	c_2	2.0
	Velocity limit	v_max	5

Parameter Category	Parameter Name	Symbol	Value
Physics Model	Minimum radius	R_min	0.01
	Maximum radius	R_max	0.5
	Radius exponent	β	1.0
	Epsilon constant	ε	1e-10

The parameter values were chosen to balance exploration and exploitation while maintaining computational efficiency. The angle quantization factor $\alpha = \pi/8$ creates 4 angular sectors for bi-objective problems, providing sufficient granularity for directional diversity without excessive computational overhead.

4. Experimental Design and Setup

4.1 Benchmark Test Problems

Six widely used bi-objective benchmark problems describing a variety of Pareto front geometries and complexity levels in multi-objective optimization studies were used to test the performance of EMOBHO-AQCD [10, 26].

The selected problems include Schaffer No.1 (SCH1) [27], Fonseca–Fleming (FON) [2], Poloni [28], Kursawe (KUR) [26], and ZDT1 and ZDT3 [10]. All these benchmarks encompass non-convex, concave, convex, and disconnected Pareto fronts, which allow the evaluation of convergence behavior, diversity preservation, and scalability properties. Table (3-5) shows the features, parameter specification, and mathematical model of the chosen benchmark problems.

Table 3 *Test problem characteristics summary*

Problem	Variables	Objectives	Pareto Front Type	Key Challenge
SCH1	1	2	Convex	Simple baseline
FON	3	2	Concave	Multi-modality
Poloni	2	2	Non-convex	Complex geometry
KUR	3	2	Disconnected	Multiple segments
ZDT1	30	2	Convex	High dimension
ZDT3	10	2	Disconnected	Five segments

Table 4 *Test problems parameters*

Test Problem	Number of Variables	Minimum	Maximum
Schaffer No.1	1	-10	+10
Fonseca-Fleming	3	-4	+4
Poloni	2	-π	+ π
Kursawe	3	-5	+5
ZDT1	30	0	+1
ZDT3	10	0	+1

Table 5 *Mathematical formulation of the characteristics of test problems*

Test Problem	Variables	Variable Range	Objective Functions	Notes / Optimal Solutions
Schaffer No.1	1	[-10, +10]	$f_1(x) = x^2$ $f_2(x) = (x-2)^2$	$f_2 = (\sqrt{f_1} - 2)^2$
Fonseca-Fleming	3	[-4, +4]	$f_1(\mathrm{x}) = 1 - \exp\left(-\sum_{i=1}^{n}\left(x_i - \frac{1}{\sqrt{n}}\right)^2\right)$ $f_2(\mathrm{x}) = 1 - \exp\left(-\sum_{i=1}^{n}\left(x_i + \frac{1}{\sqrt{n}}\right)^2\right)$	$x_j = \pm\frac{1}{\sqrt{n}}$

Test Problem	Variables	Variable Range	Objective Functions	Notes / Optimal Solutions
Poloni	2	[-π, +π]	$f_1(\mathrm{x}) = 1 + (a_1 - b_1)^2 + (a_2 - b_2)^2$ $f_2(\mathrm{x}) = (x_1 + 3)^2 + (x_2 + 1)^2$	Complex, difficult to obtain
Kursawe	3	[-5, +5]	$f_1(\mathrm{x}) = \sum_{i=1}^{n-1} -10 \cdot \exp\left(-0.2 \cdot \sqrt{x_i^2 + x_{i+1}^2}\right)$ $f_2(\mathrm{x}) = \sum_{i=1}^{n} (\lvert x_i \rvert^{0.8} + 5 \cdot \sin(x_i^3))$	x_i
ZDT1	30	[0, 1]	$f_1(x) = x_1$ $f_2(x) = g \cdot \left(1 - \sqrt{\frac{f_1}{g}}\right)$, where $g = 1 + 9 \cdot \frac{1}{n-1} \sum_{i=2}^{n} x_i$	$x_1 \in [0,1], x_i = 0$ for $i = 2, \ldots, n$
ZDT3	10	[0, 1]	$f_1(x) = x_1$ $f_2(x) = g \cdot \left(1 - \sqrt{\frac{f_1}{g}} - \frac{f_1}{g} \cdot \sin(10\pi f_1)\right)$, where $g = 1 + 9 \cdot \frac{1}{n-1} \sum_{i=2}^{n} x_i$	$x_1 \in [0,1], x_i = 0$ for $i = 2, \ldots, n$

4.2 Performance Metrics

The analysis of multi-objective optimization algorithms is based on the need to analyze the quality of convergence and the maintenance of diversity simultaneously. As a measure of holistic assessment, eight objective performance indicators were used.

The adopted metrics include:

- Spread (Δ) [1]
- Generational Distance (GD) [29]
- Hypervolume (HV) [30]
- Overall Spread (OS)
- Set Coverage metrics (SC1 and SC2) [10]
- Uniform Distribution (UD)

Generational Distance (GD) quantifies closeness to the actual Pareto front [29], whereas Hypervolume (HV) assesses the convergence as well as diversity at the same time by quantifying the volume of the dominated objective space [30]. Distribution uniformity and boundary coverage are assessed by Spread (Δ) [1]. Set Coverage metrics measure the dominance between Pareto fronts [10]. Uniform Distribution (UD) evaluates the consistency of spacing among non-dominated solutions. Together, these metrics provide a balanced assessment of convergence, distribution quality, and dominance performance.

Table 6 *Summary of performance metrics used for multi-objective evaluation*

Metric	Purpose	Simplified Formula	Interpretation
Delta (Δ)	Measures the spread and uniformity of solutions along the Pareto front	$\Delta = \frac{d_L + d_F + \sum_{i=1}^{N-1} \lvert d_i - \bar{d} \rvert}{d_L + d_F + (N-1)\bar{d}}$	Low Δ (≈ 0) → evenly spaced solutions with good boundary coverage; High Δ (→ 1) → poor distribution, clustering, or missing boundary coverage
Delta with Interpolation (Δ_i)	Estimates diversity using interpolated boundary solutions	Same as Δ with curve-fitted boundaries	Low Δ_i → uniform distribution even when true boundary points are unavailable
Generational Distance (GD)	Measures convergence to the true Pareto front	$GD = \left(\frac{1}{N} \sum d_i^q\right)^{\frac{1}{q}}$	Lower GD → better proximity to true Pareto front

Metric	Purpose	Simplified Formula	Interpretation
Hypervolume (HV)	Quantifies both convergence and diversity via dominated volume	$HV = \sum(f_1^{(i)} - r_1)(f_2^{(i)} - r_2)$	Higher HV → better solution quality across convergence and spread
Overall Pareto Spread (OS)	Measures the coverage range of the Pareto front	$OS = \prod\left(\frac{\text{range}_S}{\text{range}_{\text{ref}}}\right)$	OS ≈ 1 → solutions cover the entire objective space
Set Coverage 1 (SC1)	Assesses how many solutions in S resist domination by R	$SC1 = \frac{N_{\text{non-dom}}}{N}$	SC1 ≈ 1 → S is competitive or better than R
Set Coverage 2 (SC2)	Measures how many solutions in S2 are dominated by S1	$SC2 = \frac{K_{\text{dom}}}{K}$	SC2 ≈ 1 → S1 strongly dominates S2
Uniform Distribution (UD)	Evaluates the evenness of solution spacing	$UD = \frac{1}{1 + D_{nc}}$	UD ≈ 1 → solutions are evenly and uniformly distributed

4.3 Experimental Protocol

4.3.1 Algorithm Selection

Four representative multi-objective optimization algorithms were selected for comparative evaluation:

- NSGA-II [1]
- NSGA-III [6]
- MOPSO [8]
- MOEA/D [31]

These algorithms represent dominance-based, reference-point–based, swarm-based, decomposition-based, and physics-inspired paradigms.
In addition, three internal variants were evaluated:

- MOBHO (baseline multi-objective black hole implementation).
- EMOBHO – energy-based extension of MOBHO.
- EMOBHO-AQCD – full proposed framework integrating energy lifecycle regulation, angle quantization [21], and crowding-distance archive management.

EMOBHO and EMOBHO-AQCD are proposed in this work as adaptive extensions of MOBHO.

4.3.2 Parameter Configuration

All the algorithms were done in MATLAB R2021a under standard conditions. All algorithms used a population size (N = 100) and a maximum number of iterations (T = 100). The size of the archive was to be A = 100 accordingly. Parameters of the algorithm are based on the suggested parameters in their original research [1, 6, 8, 31] to ensure fair comparison. Parameters of EMOBHO-AQCD, such as energy coefficient and angle quantization factor ($\alpha = \pi/8$), are listed in Table 2 (Section 3.6). Table 7 presents the algorithm parameter configuration.

Table 7 *Algorithm parameter configuration*

Parameter	NSGA-II	NSGA-III	MOPSO	MOEA/D	MOBHO	EMOBHO	EMOBHO-AQCD
			General Parameters				
Population Size	100	100	100	100	100	100	100
Max Iterations	100	100	100	100	100	100	100
Archive Size	-	-	100	100	100	100	100
			Algorithm-Specific Parameters				
Crossover Probability	0.7	0.5	-	-	-	-	-

Parameter	NSGA-II	NSGA-III	MOPSO	MOEA/D	MOBHO	EMOBHO	EMOBHO-AQCD
Mutation Probability	0.4	0.5	-	-	-	-	-
μ (Distribution Index)	0.02	0.02	-	-	-	-	-
Number of Divisions	-	10	-	-	-	-	-
Crossover Gamma	-	-	-	0.5	-	-	-
Inertia Coefficient	-	-	0.4	-	0.15	0.15	0.15
Cognitive Coefficient	-	-	2.0	-	0.30	0.30	0.30
Social Coefficient	-	-	2.0	-	0.30	0.30	0.30
Grid Size	-	-	20	-	-	-	-
Max Velocity	-	-	5	-	5	5	5
Mutation Factor	-	-	0.5	-	-	-	-
Black Hole Specific Parameters							
Number of Black Holes	-	-	-	-	5	5	5
Reassignment Period	-	-	-	-	5	5	5
Alpha (reassigned stars fraction)	-	-	-	-	10%	10%	10%

5. Results

Experiments were done under the same computational conditions. The stopping condition is 100 iterations, which equals 10,000 evaluations of the function in each run, the same as the standard benchmarking standards in multi-objective optimization [10, 29]. All algorithms were executed independently for 10 runs with different random seeds for primary performance reporting (mean and standard deviation) and paired t-test comparisons.

To enhance non-parametric validation, an additional set of 20 paired independent runs was conducted for the three proposed variants (MOBHO, EMOBHO, and EMOBHO-AQCD) for Wilcoxon signed-rank tests, effect size analysis (Cohen's d), and 95% confidence interval estimation. All statistical tests were conducted at a significance level of $\alpha = 0.05$, following established evaluation standards in multi-objective optimization benchmarking [10, 29].

5.1 Evaluation Framework, Metric Interpretation, and Set Coverage Analysis

EMOBHO-AQCD was tested on six classical bi-objective benchmark problems (SCH1, FON, POL, KUR, ZDT1, and ZDT3) with eight complementary measures of performance using ten independent runs on an algorithm. The experimental study compares three proposed variants (MOBHO, EMOBHO, and EMOBHO-AQCD) against four well-known multi-objective optimization methods (NSGA-II, NSGA-III, MOPSO, and MOEA/D). Algorithm performance metrics and parametric statistical tests were conducted across 10 independent runs for all algorithms.

To gain statistical power of non-parametric robustness analysis, 20 independent paired runs were calculated to test the proposed variants with Wilcoxon signed-rank tests. The assessment scheme incorporates dominance-based, convergence-based, and distribution-based measures: Set Coverage (SC1, SC2) to measure dominance relations, Generational Distance (GD) and Hypervolume (HV) to measure convergence quality, and Delta, Δi, Uniform Distribution Euclidean (UDE), Uniform Distribution Average (UDA), and Overall Pareto Spread (OPS) to measure distribution and spread measures. The metrics of set coverage are given the first priority since they are directly used to measure the Pareto dominance between approximation sets. SC1 is a metric of resistance to competitor domination, and SC2 is a metric of active domination of competitor solutions. These metrics are useful as they complement geometric indicators like GD and HV, as they measure dominance behavior and not just proximity. The multi-metric methodology can give an overall picture of the performance of algorithms in a wide range of front geometries and problem complexity, considering that algorithmic performance is problem-dependent, not absolute.

The set coverage analysis gives the main evaluation of the relationships between the dominance of algorithms in all the test problems. The overall findings provide a comprehensive profile of EMOBHO-AQCD compared with other algorithms and indicate specific tendencies in algorithmic efficiency across different optimization landscapes. Table 8 presents the SC1 and SC2 results for EMOBHO-AQCD compared with all competing algorithms across the six benchmark problems. At SCH1, EMOBHO-AQCD attains SC1 values of 0.998 to 1.000 compared to all competitors, which means that it is almost resistant to domination.

Table 8 *Set coverage for EMOBHO-AQCD vs. other algorithms*

TP	SC	EMOBHO	MOBHO	MOEA/D	MOPSO	NSGA-II	NSGA-III
FON	SC1	0.8351	0.9382	0.8240	0.8453	0.7874	0.8870
	SC2	0.0862	0.3522	0.0743	0.1580	0.0719	0.1091
POL	SC1	0.5402	0.7519	0.4231	0.3177	0.3055	0.3172
	SC2	0.1422	0.2324	0.0097	0.0362	0.0113	0.0174
Sch 1	SC1	0.9987	0.9986	1.0000	0.9980	0.9980	0.9991
	SC2	0.0000	0.0000	0.0000	0.0000	0.0000	0.0008
KUR	SC1	0.6497	0.8199	0.8718	0.5698	0.2836	0.4812
	SC2	0.2268	0.3717	0.5441	0.2100	0.0137	0.0424
ZDT1	SC1	0.5105	0.2251	0.2433	0.0000	0.0000	0.0000
	SC2	0.4739	0.3017	0.0000	0.0000	0.0000	0.0000
ZDT3	SC1	0.5263	0.5747	0.1239	0.0000	0.0000	0.0092
	SC2	0.4870	0.5462	0.0000	0.0000	0.0000	0.0000

The values of SC2 are quite close to zero, which indicates that mutual convergence to almost the same Pareto approximations occurs for this simple convex problem. On FON, the SC1 ranges from 0.787 to 0.938, and there is high resistance to domination; the value of SC2 is as high as 0.352 against MOBHO, which indicates the ability to dominate. In the case of POL, the values of SC1 and SC2 range between 0.306 and 0.752 and 0.232, respectively, with the highest resistance being against MOBHO, which proves active dominance on this multi-mode geometry. On KUR, EMOBHO-AQCD has the highest SC2 with MOEA/D (0.544), and all SC1 decreases when compared to NSGA-II, indicating convergence issues on disconnected geometry. In the case of ZDT1 and ZDT3, SC1 and SC2 figures against MOPSO and NSGA-II are running towards zero and not directly defeated, a result of fundamental inabilities to converge on problems of high dimensions, but not due to failure to dominate. All-set coverage results have shown that EMOBHO-AQCD consistently outperforms MOBHO across all problems and exhibits competitive dominance behavior on low- to moderate-complexity fronts.

5.2 Performance Analysis by Test Problem

5.2.1 Schaffer's Problem No.1

EMOBHO-AQCD reaches almost the optimum convergence (GD = 0.0010) on SCH1, which is similar to EMOBHO, MOBHO, and traditional MOEAs (GD = 0.0009). Hypervolume (12.0292) performs competitively with the BHO family, whereas MOEA/D has much worse coverage (HV = 7.0038). Although Delta (0.8479) is higher than MOPSO (0.3619) and NSGA-II (0.3902) in a manner that is reflective of their superiority in this simple convex geometry, EMOBHO-AQCD progressively improves over both MOBHO (0.9058) and EMOBHO (0.8825), which confirms the progressive increase in all the proposed variants. EMOBHO-AQCD (UDE = 0.1227, UDA = 0.1456) is better than MOPSO (0.2489, 0.3171) and NSGA-II (0.2475, 0.3083), as it can exhibit evenly distributed solutions within the BHO family. The detailed results are presented in Table 9.

Table 9 *Performance metrics for Schaffer's problem no.1*

Performance Metric	Statistics	EMOBHO-AQCD	EMOBHO	MOBHO	MOPSO	NSGA-II	NSGA-III	MOEA/D
Delta	μ	0.8479	0.8825	0.9058	0.3619	0.3902	0.9073	1.093
	σ	0.0438	0.0463	0.0451	0.039	0.0433	0.0453	0.0444
	σ2	0.0019	0.0021	0.002	0.0015	0.0019	0.002	0.002
Delta with Interpolation	μ	0.8613	0.8919	0.9151	0.4399	0.4639	0.9156	1.1108
	σ	0.0401	0.0425	0.0403	0.0348	0.0364	0.0437	0.0471
	σ2	0.0016	0.0018	0.0016	0.0012	0.0013	0.0019	0.0022
Generational Distance	μ	0.001	0.001	0.001	0.0009	0.0009	0.0009	0.0009
	σ	0.0001	0.0001	0.0	0.0	0.0001	0.0001	0.0
	σ2	0.0	0.0	0.0	0.0	0.0	0.0	0.0
Hyper Volume	μ	12.0292	12.4167	12.6979	13.2648	13.2535	12.0066	7.0038
	σ	1.049	0.4796	0.4096	0.0055	0.0166	1.1231	1.578
	σ2	1.1003	0.23	0.1678	0.0	0.0003	1.2613	2.4901
Overall Pareto Spread	μ	0.9254	0.9521	0.9703	1.0	0.9996	0.923	0.5876
	σ	0.0709	0.0312	0.026	0.0004	0.0011	0.0742	0.1138
	σ2	0.005	0.001	0.0007	0.0	0.0	0.0055	0.013
Uniform Distribution Euclidean	μ	0.1227	0.1693	0.1677	0.2489	0.2475	0.0793	0.0704
	σ	0.0371	0.0438	0.0297	0.0371	0.0322	0.0096	0.0169
	σ2	0.0014	0.0019	0.0009	0.0014	0.001	0.0001	0.0003
Uniform Distribution Average	μ	0.1456	0.194	0.1956	0.3171	0.3083	0.1037	0.089
	σ	0.0388	0.0453	0.0355	0.0447	0.0361	0.0126	0.025
	σ2	0.0015	0.0021	0.0013	0.002	0.0013	0.0002	0.0006

T-test comparison demonstrates that there is a significant improvement over MOBHO on Delta ($p = 0.0094$) and UDE/UDA ($p < 0.01$) and no significant difference between EMOBHO-AQCD and EMOBHO on convergence measures (GD $p = 0.9015$, HV $p = 0.302$), as shown in Tables (10-11).

Table 10 *T-test for Schaffer's problem no. 1 (part 1)*

Metric	T-Test	emobhoaqcd emobho	emobhoaqcd mobho	emobhoaqcd mopso	emobhoaqcd nsga2	emobhoaqcd nsga3	emobhoaqcd moead	emobho mobho	emobho mopso	emobho nsga2	emobho nsga3
Delta	p	0.1031	0.0094	0.0	0.0	0.008	0.0	0.2708	0.0	0.0	0.2423
	h	0.0	1.0	1.0	1.0	1.0	1.0	0.0	1.0	1.0	0.0
Delta w/I	p	0.1154	0.0079	0.0	0.0	0.0096	0.0	0.227	0.0	0.0	0.2338
	h	0.0	1.0	1.0	1.0	1.0	1.0	0.0	1.0	1.0	0.0
GD	p	0.9015	0.751	0.6255	0.8483	0.4408	0.0438	0.403	0.5115	0.913	0.2957
	h	0.0	0.0	0.0	0.0	0.0	1.0	0.0	0.0	0.0	0.0
HV	p	0.302	0.0767	0.0015	0.0017	0.9634	0.0	0.1756	0.0	0.0	0.3022
	h	0.0	0.0	1.0	1.0	0.0	1.0	0.0	1.0	1.0	0.0
OS	p	0.2909	0.0765	0.0037	0.0039	0.9426	0.0	0.173	0.0001	0.0001	0.269
	h	0.0	0.0	1.0	1.0	0.0	1.0	0.0	1.0	1.0	0.0
UD Euc	p	0.0194	0.0078	0.0	0.0	0.0021	0.0008	0.9224	0.0004	0.0003	0.0
	h	1.0	1.0	1.0	1.0	1.0	1.0	0.0	1.0	1.0	1.0
UD Avg	p	0.0196	0.0076	0.0	0.0	0.0044	0.0011	0.9286	0.0	0.0	0.0
	h	1.0	1.0	1.0	1.0	1.0	1.0	0.0	1.0	1.0	1.0

Table 11 presents the remaining pairwise T-test comparisons for SCH1.

Table 11 T-test for Schaffer's problem no.1 (part 2)

Metric	T-Test	emobho moead	mobho mopso	mobho nsga2	mobho nsga3	mobho moead	mopso nsga2	mopso nsga3	mopso moead	nsga2 nsga3	nsga2 moead	nsga3 moead
Delta	p	0.0	0.0	0.0	0.9408	0.0	0.1428	0.0	0.0	0.0	0.0	0.0
	h	1.0	1.0	1.0	0.0	1.0	0.0	1.0	1.0	1.0	1.0	1.0
Delta w/I	p	0.0	0.0	0.0	0.9762	0.0	0.1502	0.0	0.0	0.0	0.0	0.0
	h	1.0	1.0	1.0	0.0	1.0	0.0	1.0	1.0	1.0	1.0	1.0
GD	p	0.0009	0.0439	0.2868	0.0416	0.0	0.5537	0.5318	0.0001	0.3112	0.0004	0.02
	h	1.0	1.0	0.0	1.0	1.0	0.0	0.0	1.0	0.0	1.0	1.0
HV	p	0.0	0.0004	0.0004	0.0841	0.0	0.0565	0.0023	0.0	0.0025	0.0	0.0
	h	1.0	1.0	1.0	0.0	1.0	0.0	1.0	1.0	1.0	1.0	1.0
OS	p	0.0	0.002	0.0023	0.0734	0.0	0.22	0.0041	0.0	0.0043	0.0	0.0
	h	1.0	1.0	1.0	0.0	1.0	0.0	1.0	1.0	1.0	1.0	1.0
UD Euc	p	0.0	0.0	0.0	0.0	0.0	0.9283	0.0	0.0	0.0	0.0	0.1687
	h	1.0	1.0	1.0	1.0	1.0	0.0	1.0	1.0	1.0	1.0	0.0
UD Avg	p	0.0	0.0	0.0	0.0	0.0	0.6328	0.0	0.0	0.0	0.0	0.1156
	h	1.0	1.0	1.0	1.0	1.0	0.0	1.0	1.0	1.0	1.0	0.0

Wilcoxon signed-rank test (20 paired runs) versus MOBHO validates significant improvements on HV ($p = 0.0124$, $d = +0.713$, medium), Delta ($p = 0.0137$, $d = -0.818$, large), Delta w/I ($p = 0.0152$, $d = -0.786$, medium), and UDA ($p = 0.0124$, $d = -0.791$, medium), in which the gains are significant without degradation of convergence. There is no comparison to classical MOEAs since the GD fluctuation among all algorithms in this problem (floor effect) is insignificant. Table 12 presents the Wilcoxon signed-rank test for SCH1.

Table 12 *Wilcoxon signed-rank test for SCH1*

Metric	AQCD vs EMOBHO (p)	Cohen's d	Effect	Significant	AQCD vs MOBHO (p)	Cohen's d	Effect	Significant
GD	—	—	—	—	0.1560	-0.463	Small	—
HV	—	—	—	—	0.0124	+0.713	Medium	✓
Delta	—	—	—	—	0.0137	-0.818	Large	✓
Delta w/I	—	—	—	—	0.0152	-0.786	Medium	✓
OPS	—	—	—	—	0.3905	+0.399	Small	—
UDE	—	—	—	—	0.3905	+0.287	Small	—
UDA	—	—	—	—	0.0124	-0.791	Medium	✓

As can be seen in Fig. 2, all the algorithms approach the analytical front closely, yet EMOBHO-AQCD has a more homogenous distribution of solutions than both MOBHO and EMOBHO, in line with the quantitative improvements demonstrated in Tables 9-12.

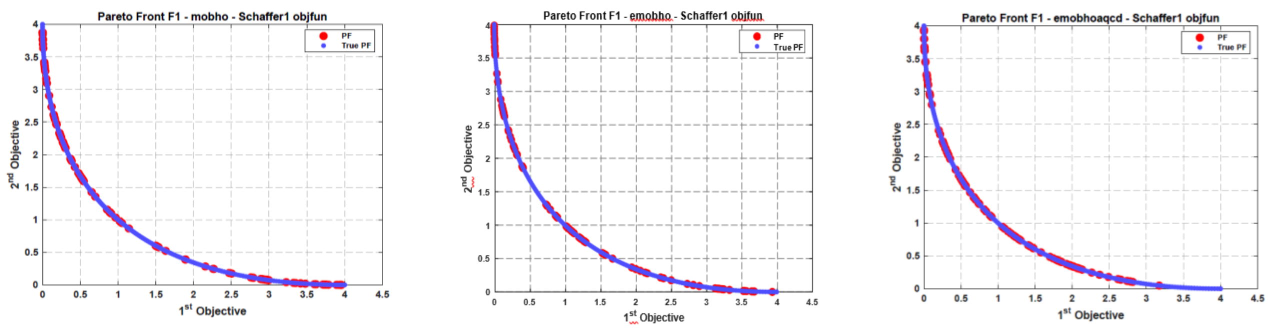

(a) (b) (c)

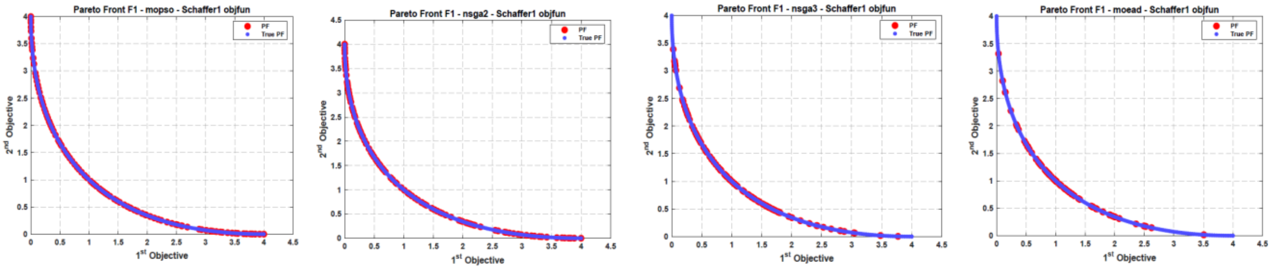

(d) (e) (f) (g)

Fig. 2 *Schaffer's problem comparison of the seven algorithms (a) EMOBHO; (b) MOBHO; (c) EMOBHO-AQCD; (d) MOPSO; (e) NSGA-II; (f) NSGA-III; (g) MOEA/D*

5.2.2 Fonseca-Fleming Problem

Competitive convergence (GD = 0.0013) is obtained when EMOBHO-AQCD is used, which is also comparable to MOPSO and NSGA-II (GD = 0.0012), and much better than MOBHO (GD = 0.0034). The value of Hypervolume (0.2097) and OPS (0.6211), however, are less than EMOBHO (0.2765, 0.8942) and MOPSO (0.2959, 0.9538), which implies a convergence-diversity trade-off on this concave geometry. Even though Delta (0.7848) is higher than MOPSO (0.2732) and NSGA-II (0.3434), reflecting their advantage on this concave geometry, EMOBHO-AQCD is still better than MOBHO (1.0529). Compared to MOPSO (0.2752, 0.3654) and NSGA-II (0.2600, 0.3258), EMOBHO-AQCD (UDE = 0.1258, UDA = 0.1484) has a more even distribution of solutions within the BHO family. Table 13 presents the performance metrics for Fonseca-Fleming's problem.

Table 13 *Performance metrics for Fonseca-Fleming's problem*

Performance Metric	Statistics	EMOBHO-AQCD	EMOBHO	MOBHO	MOPSO	NSGA-II	NSGA-III	MOEA/D
Delta	μ	0.7848	0.7797	1.0529	0.2732	0.3434	0.8798	1.0156
	σ	0.0866	0.0371	0.3279	0.0243	0.0287	0.1184	0.04
	σ2	0.0075	0.0014	0.1075	0.0006	0.0008	0.014	0.0016
Delta with Inter.	μ	0.7389	0.7828	1.073	0.3041	0.3713	0.8812	1.0182
	σ	0.1005	0.0381	0.3542	0.0237	0.0278	0.118	0.0427
	σ2	0.0101	0.0015	0.1254	0.0006	0.0008	0.0139	0.0018
Generational Distance	μ	0.0013	0.0012	0.0034	0.0012	0.0012	0.0011	0.0015
	σ	0.0001	0.0001	0.0057	0.0	0.0	0.0001	0.0006
	σ2	0.0	0.0	0.0	0.0	0.0	0.0	0.0
Hyper Volume	μ	0.2097	0.2765	0.2436	0.2959	0.2929	0.2722	0.2593
	σ	0.0358	0.0129	0.0755	0.0022	0.0053	0.0102	0.0119
	σ2	0.0013	0.0002	0.0057	0.0	0.0	0.0001	0.0001
Overall Pareto Spread	μ	0.6211	0.8942	0.8568	0.9538	0.9486	0.9159	0.7921
	σ	0.1215	0.0493	0.2011	0.0094	0.0147	0.0244	0.0987
	σ2	0.0148	0.0024	0.0404	0.0001	0.0002	0.0006	0.0097
Uniform Dist. Euc.	μ	0.1258	0.1658	0.1426	0.2752	0.26	0.0893	0.1471
	σ	0.033	0.024	0.0526	0.0221	0.025	0.0343	0.0561
	σ2	0.0011	0.0006	0.0028	0.0005	0.0006	0.0012	0.0031
Uniform Dist. Avg	μ	0.1484	0.1983	0.1618	0.3654	0.3258	0.1072	0.1725
	σ	0.0331	0.0284	0.071	0.0327	0.0269	0.0401	0.0553
	σ2	0.0011	0.0008	0.005	0.0011	0.0007	0.0016	0.0031

The analysis of the T-test proves that it has a significant improvement compared to MOBHO in Delta ($p = 0.0223$) and OS ($p = 0.0053$). EMOBHO is much more effective than EMOBHO-AQCD on GD ($p = 0.030$), HV, and OPS ($p < 0.001$), which proves the convergence-diversity trade-off on this concave geometry, as shown in Tables 14-15.

Table 14 *T-test for Fonseca-Fleming's problem (part 1)*

Metric	T-Test	emobhoaqcd emobho	emobhoaqcd mobho	emobhoaqcd mopso	emobhoaqcd nsga2	emobhoaqcd nsga3	emobhoaqcd moead	emobho mobho	emobho mopso	emobho nsga2	emobho nsga3
Delta	p	0.8662	0.0223	0.0	0.0	0.0552	0.0	0.0174	0.0	0.0	0.02
	h	0.0	1.0	1.0	1.0	0.0	1.0	1.0	1.0	1.0	1.0
Delta w/I	p	0.2131	0.0102	0.0	0.0	0.0095	0.0	0.019	0.0	0.0	0.0218
	h	0.0	1.0	1.0	1.0	1.0	1.0	1.0	1.0	1.0	1.0
GD	p	0.03	0.2718	0.003	0.001	0.0	0.3511	0.2494	0.4071	0.1476	0.0
	h	1.0	0.0	1.0	1.0	1.0	0.0	0.0	0.0	0.0	1.0
HV	p	0.0	0.2157	0.0	0.0	0.0	0.0006	0.1906	0.0002	0.0016	0.4163
	h	1.0	0.0	1.0	1.0	1.0	1.0	0.0	1.0	1.0	0.0
OS	p	0.0	0.0053	0.0	0.0	0.0	0.0028	0.5744	0.0015	0.0036	0.229
	h	1.0	1.0	1.0	1.0	1.0	1.0	0.0	1.0	1.0	0.0
UD Euc	p	0.0062	0.4057	0.0	0.0	0.0258	0.315	0.2199	0.0	0.0	0.0
	h	1.0	0.0	1.0	1.0	1.0	0.0	0.0	1.0	1.0	1.0
UD Avg	p	0.002	0.5955	0.0	0.0	0.0222	0.2513	0.1481	0.0	0.0	0.0
	h	1.0	0.0	1.0	1.0	1.0	0.0	0.0	1.0	1.0	1.0

Table 15 presents the remaining pairwise T-test comparisons for FON.

Table 15 *T-test for Fonseca-Fleming's problem (part 2)*

Metric	T-Test	emobho moead	mobho mopso	mobho nsga2	mobho nsga3	mobho moead	mopso nsga2	mopso nsga3	mopso moead	nsga2 nsga3	nsga2 moead	nsga3 moead
Delta	p	0.0	0.0	0.0	0.1339	0.7252	0.0	0.0	0.0	0.0	0.0	0.0029
	h	1.0	1.0	1.0	0.0	0.0	1.0	1.0	1.0	1.0	1.0	1.0
Delta w/I	p	0.0	0.0	0.0	0.1216	0.6326	0.0	0.0	0.0	0.0	0.0	0.0029
	h	1.0	1.0	1.0	0.0	0.0	1.0	1.0	1.0	1.0	1.0	1.0
GD	p	0.1433	0.2447	0.2411	0.2143	0.3157	0.0948	0.0	0.1131	0.0	0.095	0.022
	h	0.0	0.0	0.0	0.0	0.0	0.0	1.0	0.0	1.0	0.0	1.0
HV	p	0.006	0.0419	0.054	0.2504	0.5234	0.1162	0.0	0.0	0.0	0.0	0.0181
	h	1.0	1.0	0.0	0.0	0.0	0.0	1.0	1.0	1.0	1.0	1.0
OS	p	0.009	0.1448	0.167	0.3682	0.3735	0.3578	0.0002	0.0001	0.0019	0.0001	0.0012
	h	1.0	0.0	0.0	0.0	0.0	0.0	1.0	1.0	1.0	1.0	1.0
UD Euc	p	0.3456	0.0	0.0	0.0152	0.8536	0.1674	0.0	0.0	0.0	0.0	0.0123
	h	0.0	1.0	1.0	1.0	0.0	0.0	1.0	1.0	1.0	1.0	1.0
UD Avg	p	0.2056	0.0	0.0	0.0486	0.7099	0.0084	0.0	0.0	0.0	0.0	0.0073
	h	0.0	1.0	1.0	1.0	0.0	1.0	1.0	1.0	1.0	1.0	1.0

Wilcoxon analysis (20 paired runs) validates that EMOBHO is better than EMOBHO-AQCD on HV ($p = 0.0002$, $d = -1.206$, large) and OS ($p = 0.0039$, $d = -1.965$, large), as shown in Table 16. But EMOBHO-AQCD has better results on UDE ($p = 0.0004$, $d = -1.159$, large) and UDA Compared to MOBHO, EMOBHO-AQCD captures high returns on OS ($p = 0.0371$, $d = -0.803$, large), UDE ($p = 0.0008$, $d = -1.129$, large), and UDA ($p = 0.0090$, $d = -0.747$, medium) gain.

Table 16 *Wilcoxon signed-rank test for FON*

Metric	AQCD vs EMOBHO (p)	Cohen's d	Effect	Significant	AQCD vs MOBHO (p)	Cohen's d	Effect	Significant
HV	0.0002	-1.206	Large	✓	0.1913	-0.148	Negligible	—
GD	0.0022	+0.718	Medium	✓	0.7369	+0.041	Negligible	—
Delta	0.0228	+0.573	Medium	✓	0.2790	+0.131	Small	—
Delta w/I	0.0090	+0.691	Medium	✓	0.5755	-0.024	Negligible	—
OS	0.0039	-1.965	Large	✓	0.0371	-0.803	Large	✓

Metric	AQCD vs EMOBHO (p)	Cohen's d	Effect	Significant	AQCD vs MOBHO (p)	Cohen's d	Effect	Significant
UDE	0.0004	-1.159	Large	✓	0.0008	-1.129	Large	✓
UDA	0.0001	-1.490	Large	✓	0.0090	-0.747	Medium	✓

Fig. 3 shows that EMOBHO-AQCD can trace through the concave front with an increased internal spacing, although it reduces the full-front coverage compared to MOPSO and NSGA-II, which shows a definite convergence-diversity trade-off on this concave geometry.

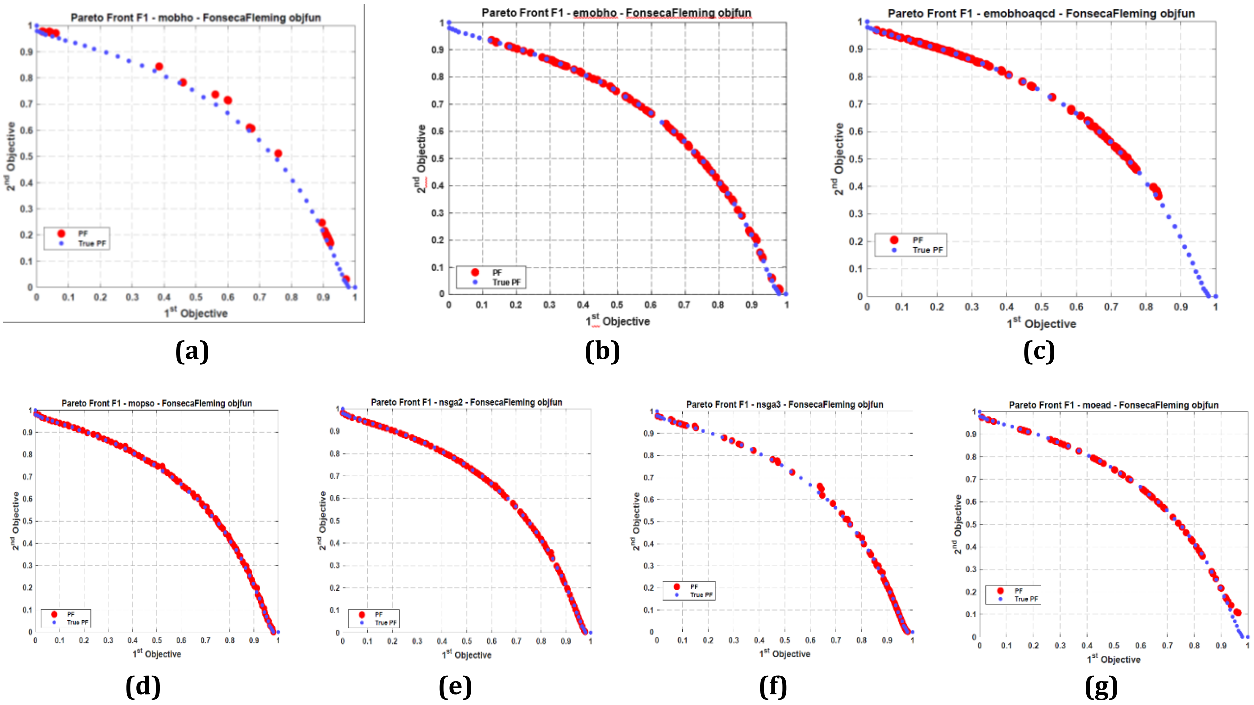

Fig. 3 *Fonseca-Fleming's problem comparison of the seven algorithms (a) EMOBHO; (b) MOBHO; (c) EMOBHO-AQCD; (d) MOPSO; (e) NSGA-II; (f) NSGA-III; (g) MOEA/D*

5.2.3 Poloni's Problem

EMOBHO-AQCD has moderate convergence (GD = 0.0407), better than MOBHO (0.0520) but worse than NSGA-III (0.0011) and MOPSO (0.0091), as shown in Table 17. Classical MOEAs demonstrate better coverage on a global scale, with Hypervolume (320.19) being smaller than MOPSO (368.96) and NSGA-II (367.64). Among the BHO family, however, EMOBHO-AQCD has the best distribution performance with the lowest UDE (0.0612) and competitive UDA (0.0631) and better Delta (1.2767) than MOBHO (1.548), which is substantiated by the fact that spacing and branch coverage are improved on this multi-modal geometry.

Table 17 *Performance metrics for Poloni's problem*

Performance Metric	Statistics	EMOBHO-AQCD	EMOBHO	MOBHO	MOPSO	NSGA-II	NSGA-III	MOEA/D
Delta	μ	1.2767	1.3517	1.548	0.9587	0.9671	1.3329	1.3632
	σ	0.0586	0.0934	0.0658	0.022	0.0281	0.048	0.2169
	σ2	0.0034	0.0087	0.0043	0.0005	0.0008	0.0023	0.047
Delta with Inter.	μ	1.2388	1.2941	1.5056	0.9681	0.9745	1.2559	1.4798
	σ	0.0538	0.0878	0.083	0.0169	0.0218	0.0424	0.1139
	σ2	0.0029	0.0077	0.0069	0.0003	0.0005	0.0018	0.013
Generational Distance	μ	0.0407	0.0333	0.052	0.0091	0.0077	0.0011	0.007
	σ	0.0226	0.0191	0.0237	0.0124	0.0132	0.0002	0.0113

Performance Metric	Statistics	EMOBHO-AQCD	EMOBHO	MOBHO	MOPSO	NSGA-II	NSGA-III	MOEA/D
	σ2	0.0005	0.0004	0.0006	0.0002	0.0002	0.0	0.0001
Hyper Volume	μ	320.1869	353.498	353.5139	368.9634	367.6399	291.9605	163.6685
	σ	45.7005	22.3448	30.7821	18.2261	19.2153	17.007	136.3119
	σ2	2088.5386	499.2922	947.538	332.1892	369.2263	289.2383	18580.9448
Overall Pareto Spread	μ	0.9221	0.9893	1.0118	1.0083	1.0051	0.812	0.4689
	σ	0.1211	0.0554	0.0716	0.0455	0.048	0.0432	0.3758
	σ2	0.0147	0.0031	0.0051	0.0021	0.0023	0.0019	0.1413
Uniform Dist. Euc.	μ	0.0612	0.0662	0.0624	0.1321	0.1417	0.054	0.0428
	σ	0.0229	0.0295	0.0385	0.0214	0.0172	0.0094	0.0115
	σ2	0.0005	0.0009	0.0015	0.0005	0.0003	0.0001	0.0001
Uniform Dist. Avg	μ	0.0631	0.0717	0.0698	0.1906	0.2034	0.0612	0.049
	σ	0.0213	0.0328	0.0428	0.0302	0.0244	0.0098	0.0203
	σ2	0.0005	0.0011	0.0018	0.0009	0.0006	0.0001	0.0004

The results of the T-test analysis indicate that there are a number of statistical differences between algorithms. EMOBHO-AQCD is significantly better than MOBHO on Delta ($p = 0.0452$), as shown in Tables 18-19.

Significant differences are found between EMOBHO-AQCD and classical MOEAs on convergence measures (GD and HV) due to the variation in search behavior between BHO-based and classical evolutionary algorithms.

Table 18 *T-test for Poloni's problem (part 1)*

Metric	T-Test	emobhoaqcd emobho	emobhoaqcd mobho	emobhoaqcd mopso	emobhoaqcd nsga2	emobhoaqcd nsga3	emobhoaqcd moead	emobho mobho	emobho mopso	emobho nsga2	emobho nsga3
Delta	p	0.0452	0.0	0.0	0.0	0.0305	0.2392	0.0	0.0	0.0	0.5786
	h	1.0	1.0	1.0	1.0	1.0	0.0	1.0	1.0	1.0	0.0
Delta w/I	p	0.1066	0.0	0.0	0.0	0.4387	0.0	0.0	0.0	0.0	0.2318
	h	0.0	1.0	1.0	1.0	0.0	1.0	1.0	1.0	1.0	0.0
GD	p	0.4437	0.2877	0.0011	0.0009	0.0	0.0005	0.0679	0.0034	0.0026	0.0
	h	0.0	0.0	1.0	1.0	1.0	1.0	0.0	1.0	1.0	1.0
HV	p	0.053	0.0718	0.0057	0.0072	0.0838	0.0029	0.999	0.1071	0.1465	0.0
	h	0.0	0.0	1.0	1.0	0.0	1.0	0.0	0.0	0.0	1.0
OS	p	0.128	0.059	0.0495	0.0591	0.0145	0.0019	0.442	0.4136	0.5034	0.0
	h	0.0	0.0	1.0	0.0	1.0	1.0	0.0	0.0	0.0	1.0
UD Euc	p	0.6772	0.9324	0.0	0.0	0.368	0.0353	0.8078	0.0	0.0	0.2276
	h	0.0	0.0	1.0	1.0	0.0	1.0	0.0	1.0	1.0	0.0
UD Avg	p	0.4969	0.6604	0.0	0.0	0.8037	0.1458	0.916	0.0	0.0	0.3473
	h	0.0	0.0	1.0	1.0	0.0	0.0	0.0	1.0	1.0	0.0

Table 19 presents the remaining pairwise T-test comparisons for POL.

Table 19 *T-test for Poloni's problem (part 2)*

Metric	T-Test	emobho moead	mobho mopso	mobho nsga2	mobho nsga3	mobho moead	mopso nsga2	mopso nsga3	mopso moead	nsga2 nsga3	nsga2 moead	nsga3 moead
Delta	p	0.88	0.0	0.0	0.0	0.0189	0.4643	0.0	0.0	0.0	0.0	0.6722
	h	0.0	1.0	1.0	1.0	1.0	0.0	1.0	1.0	1.0	1.0	0.0
Delta w/I	p	0.0007	0.0	0.0	0.0	0.5698	0.4738	0.0	0.0	0.0	0.0	0.0
	h	1.0	1.0	1.0	1.0	0.0	0.0	1.0	1.0	1.0	1.0	1.0
GD	p	0.0014	0.0001	0.0001	0.0	0.0	0.8124	0.0583	0.7034	0.1357	0.9043	0.1179
	h	1.0	1.0	1.0	1.0	1.0	0.0	0.0	0.0	0.0	0.0	0.0
HV	p	0.0004	0.1889	0.2342	0.0	0.0004	0.8762	0.0	0.0002	0.0	0.0002	0.0085
	h	1.0	0.0	0.0	1.0	1.0	0.0	1.0	1.0	1.0	1.0	1.0
OS	p	0.0004	0.8968	0.8094	0.0	0.0003	0.8823	0.0	0.0003	0.0	0.0003	0.0102
	h	1.0	0.0	0.0	1.0	1.0	0.0	1.0	1.0	1.0	1.0	1.0
UD Euc	p	0.0309	0.0001	0.0	0.5083	0.1387	0.2855	0.0	0.0	0.0	0.0	0.0276
	h	1.0	1.0	1.0	0.0	0.0	0.0	1.0	1.0	1.0	1.0	1.0
UD Avg	p	0.0789	0.0	0.0	0.5423	0.18	0.313	0.0	0.0	0.0	0.0	0.102
	h	0.0	1.0	1.0	0.0	0.0	0.0	1.0	1.0	1.0	1.0	0.0

Wilcoxon analysis (20 paired runs) confirms significant improvement over MOBHO when compared to MOBHO on Delta ($p = 0.0007$, $d = -1.045$, large) and Delta w/I ($p = 0.0007$, $d = -1.003$, large). On GD, a borderline significant difference is found against EMOBHO ($p = 0.0195$, $d = +1.006$, large) in favor of EMOBHO, consistent with the convergence-diversity trade-off observed on FON. There is no significant difference between EMOBHO-AQCD and EMOBHO on the rest of the metrics. Table 20 shows the Wilcoxon signed-rank test for Ploloni.

Table 20 *Wilcoxon signed-rank test for Ploloni*

Metric	AQCD vs EMOBHO (p)	Cohen's d	Effect	Significant	AQCD vs MOBHO (p)	Cohen's d	Effect	Significant
HV	0.7652	-0.063	Negligible	—	0.8228	-0.037	Negligible	—
GD	0.0195	+1.006	Large	✓	0.8457	+0.025	Negligible	—
Delta	0.4553	-0.376	Small	—	0.0007	-1.045	Large	✓
Delta w/I	0.9108	-0.048	Negligible	—	0.0007	-1.003	Large	✓
OS	0.3223	-0.234	Small	—	0.1055	-0.424	Small	—
UDE	0.6274	+0.085	Negligible	—	0.7938	+0.097	Negligible	—
UDA	0.1454	-0.288	Small	—	0.9108	+0.081	Negligible	—

Fig. 4 shows that EMOBHO-AQCD has the broadest coverage in the BHO family as it extends into the curved upper section as well as the lower branch, but NSGA-III is the closest on the global level to the true front.

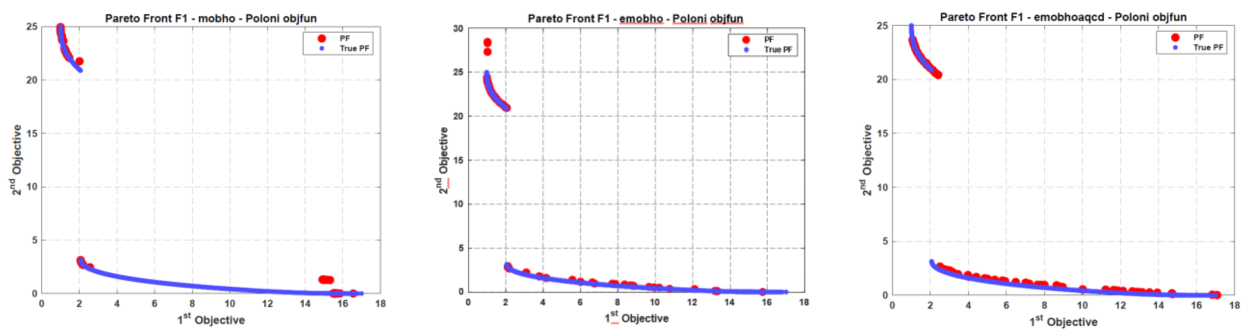

(a) (b) (c)

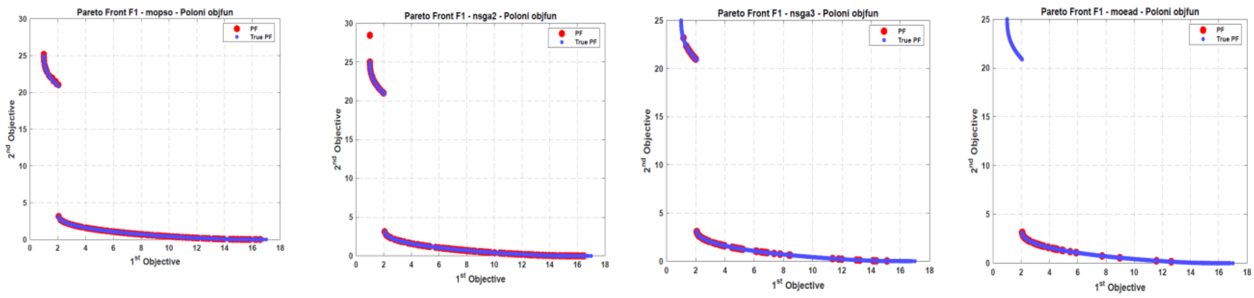

(d) **(e)** **(f)** **(g)**

Fig.4 *Poloni's problem comparison of the seven algorithms (a) EMOBHO; (b) MOBHO; (c) EMOBHO-AQCD; (d) MOPSO; (e) NSGA-II; (f) NSGA-III; (g) MOEA/D*

5.2.4 Kursawe's Problem

EMOBHO-AQCD shows mixed performance at the discontinuous three-segment KUR front. Quality convergence (GD = 0.0157) is significantly better than MOBHO (0.0325) but not as great as NSGA-II (0.0068) and NSGA-III (0.0074). Hypervolume (20.97) is smaller than EMOBHO (26.99), MOPSO (25.79), and NSGA-II (25.19), reflecting reduced global coverage on this disconnected geometry. Although these coverage limitations exist, EMOBHO-AQCD retains competitiveness in terms of spacing characteristics with the BHO family (UDE = 0.0993, UDA = 0.1243), which is similar to EMOBHO and better when compared to MOBHO. The detailed results are shown in Table 21.

Table 21 *Performance metrics for Kursawe's problem*

Performance Metric	Statistics	EMOBHO-AQCD	EMOBHO	MOBHO	MOPSO	NSGA-II	NSGA-III	MOEA/D
Delta	μ	1.0415	0.9851	1.3597	0.6666	0.4883	0.8631	1.2434
	σ	0.1084	0.0441	0.0627	0.041	0.0171	0.0595	0.118
	σ2	0.0118	0.0019	0.0039	0.0017	0.0003	0.0035	0.0139
Delta with Inter.	μ	1.0461	0.9841	1.4279	0.6655	0.49	0.8619	1.5005
	σ	0.1282	0.0458	0.1619	0.0417	0.0157	0.0605	0.2384
	σ2	0.0164	0.0021	0.0262	0.0017	0.0002	0.0037	0.0568
Generational Distance	μ	0.0157	0.0151	0.0325	0.0106	0.0068	0.0074	0.0312
	σ	0.0023	0.0037	0.02	0.0011	0.0004	0.0011	0.0197
	σ2	0.0	0.0	0.0004	0.0	0.0	0.0	0.0004
Hyper Volume	μ	20.9693	26.9873	25.8998	25.7939	25.1946	23.8238	6.229
	σ	3.8517	4.7934	11.9178	1.0497	0.5853	0.8054	5.1312
	σ2	14.8358	22.9768	142.0348	1.1019	0.3426	0.6486	26.3289
Overall Pareto Spread	μ	0.6558	0.8437	0.8058	0.8714	0.8803	0.8543	0.2434
	σ	0.1163	0.0883	0.2159	0.0165	0.0114	0.0202	0.1836
	σ2	0.0135	0.0078	0.0466	0.0003	0.0001	0.0004	0.0337
Uniform Dist. Euc.	μ	0.0993	0.0982	0.1033	0.1341	0.2614	0.1399	0.0799
	σ	0.0288	0.0274	0.0436	0.028	0.0237	0.0389	0.0311
	σ2	0.0008	0.0008	0.0019	0.0008	0.0006	0.0015	0.001
Uniform Dist. Avg	μ	0.1243	0.1241	0.1079	0.1732	0.3006	0.152	0.0979
	σ	0.0263	0.0407	0.0356	0.035	0.0138	0.0268	0.0428
	σ2	0.0007	0.0017	0.0013	0.0012	0.0002	0.0007	0.0018

The results of the T-tests show that EMOBHO-AQCD is considerably weaker than EMOBHO on HV (p = 0.006) and OS (p = 0.001), and notably weaker than MOPSO and NSGA-II on Delta, GD, and HV (p < 0.01). There is no pronounced difference between EMOBHO-AQCD and EMOBHO in the spacing metrics (UDE, UDA) (see Tables 22-23).

Table 22 *T-test for Kursawe's problem (part 1)*

Metric	T-Test	emobhoaqcd emobho	emobhoaqcd mobho	emobhoaqcd mopso	emobhoaqcd nsga2	emobhoaqcd nsga3	emobhoaqcd moead	emobho mobho	emobho mopso	emobho nsga2	emobho nsga3
Delta	p	0.1449	0.0	0.0	0.0	0.0002	0.0009	0.0	0.0	0.0	0.0001
	h	0.0	1.0	1.0	1.0	1.0	1.0	1.0	1.0	1.0	1.0
Delta w/I	p	0.1667	0.0	0.0	0.0	0.0007	0.0	0.0	0.0	0.0	0.0001
	h	0.0	1.0	1.0	1.0	1.0	1.0	1.0	1.0	1.0	1.0

GD	p	0.6707	0.0165	0.0	0.0	0.0	0.0237	0.0143	0.0017	0.0	0.0
	h	0.0	1.0	1.0	1.0	1.0	1.0	1.0	1.0	1.0	1.0
HV	p	0.0063	0.2292	0.0012	0.003	0.034	0.0	0.792	0.4518	0.2557	0.0544
	h	1.0	0.0	1.0	1.0	1.0	1.0	0.0	0.0	0.0	0.0
OS	p	0.0007	0.069	0.0	0.0	0.0	0.0	0.613	0.3434	0.2105	0.7172
	h	1.0	0.0	1.0	1.0	1.0	1.0	0.0	0.0	0.0	0.0
UD Euc	p	0.9285	0.8132	0.0136	0.0	0.0163	0.1641	0.7575	0.0096	0.0	0.0126
	h	0.0	0.0	1.0	1.0	1.0	0.0	0.0	1.0	1.0	1.0
UD Avg	p	0.9933	0.2567	0.0024	0.0	0.0314	0.1139	0.3535	0.0097	0.0	0.0872
	h	0.0	0.0	1.0	1.0	1.0	0.0	0.0	1.0	1.0	0.0

Table 23 presents the remaining pairwise T-test comparisons for KUR.

Table 23 *T-test for Kursawe's problem (part 2)*

Metric	T-Test	emobho moead	mobho mopso	mobho nsga2	mobho nsga3	mobho moead	mopso nsga2	mopso nsga3	mopso moead	nsga2 nsga3	nsga2 moead	nsga3 moead
Delta	p	0.0	0.0	0.0	0.0	0.0131	0.0	0.0	0.0	0.0	0.0	0.0
	h	1.0	1.0	1.0	1.0	1.0	1.0	1.0	1.0	1.0	1.0	1.0
Delta w/I	p	0.0	0.0	0.0	0.0	0.4361	0.0	0.0	0.0	0.0	0.0	0.0
	h	1.0	1.0	1.0	1.0	0.0	1.0	1.0	1.0	1.0	1.0	1.0
GD	p	0.0205	0.0028	0.0007	0.0009	0.8819	0.0	0.0	0.0039	0.0966	0.001	0.0013
	h	1.0	1.0	1.0	1.0	0.0	1.0	1.0	1.0	0.0	1.0	1.0
HV	p	0.0	0.978	0.8538	0.5894	0.0001	0.1322	0.0002	0.0	0.0004	0.0	0.0
	h	1.0	0.0	0.0	0.0	1.0	0.0	1.0	1.0	1.0	1.0	1.0
OS	p	0.0	0.3507	0.2901	0.4884	0.0	0.1763	0.0531	0.0	0.0023	0.0	0.0
	h	1.0	0.0	0.0	0.0	1.0	0.0	0.0	1.0	1.0	1.0	1.0
UD Euc	p	0.1798	0.0767	0.0	0.0632	0.184	0.0	0.7053	0.0007	0.0	0.0	0.0013
	h	0.0	0.0	1.0	0.0	0.0	1.0	0.0	1.0	1.0	1.0	1.0
UD Avg	p	0.1763	0.0006	0.0	0.0057	0.577	0.0	0.1442	0.0004	0.0	0.0	0.0033
	h	0.0	1.0	1.0	1.0	0.0	1.0	0.0	1.0	1.0	1.0	1.0

In Table 24, Wilcoxon signed-rank analysis (20 paired runs) proves that EMOBHO is much better than EMOBHO-AQCD at HV ($p = 0.0152$, $d = -0.528$, medium effect), GD ($p = 0.0366$, $d = +0.518$, medium effect), and Delta ($p = 0.0152$, $d = +0.613$, medium effect). MOBHO is also better than EMOBHO-AQCD on HV ($p = 0.0090$, $d = -0.605$, medium effect) and OS ($p = 0.0025$, $d = -0.717$, medium effect). There is no major difference between EMOBHO-AQCD and MOBHO in terms of spacing (UDE, UDA), which confirms that the two exhibit similar behaviour with regard to distribution.

Table 24 *Wilcoxon signed-rank test for Kursawe*

Metric	AQCD vs EMOBHO (p)	Cohen's d	Effect	Significant	AQCD vs MOBHO (p)	Cohen's d	Effect	Significant
HV	0.0152	-0.528	Medium	✓	0.0090	-0.605	Medium	✓
GD	0.0366	+0.518	Medium	✓	0.6274	+0.059	Negligible	—
Delta	0.0152	+0.613	Medium	✓	0.4115	-0.191	Small	—
Delta w/I	0.0731	+0.441	Small	—	0.9108	-0.006	Negligible	—
OS	0.0731	-0.464	Small	—	0.0025	-0.717	Medium	✓
UDE	0.9405	+0.020	Negligible	—	0.1454	-0.277	Small	—
UDA	0.9702	+0.058	Negligible	—	0.1560	-0.382	Small	—

Figure 5 confirms that EMOBHO-AQCD is able to detect all three disconnected segments, which is a testament to the fact that the discontinuous Pareto structures are well handled even with lower global coverage than EMOBHO.

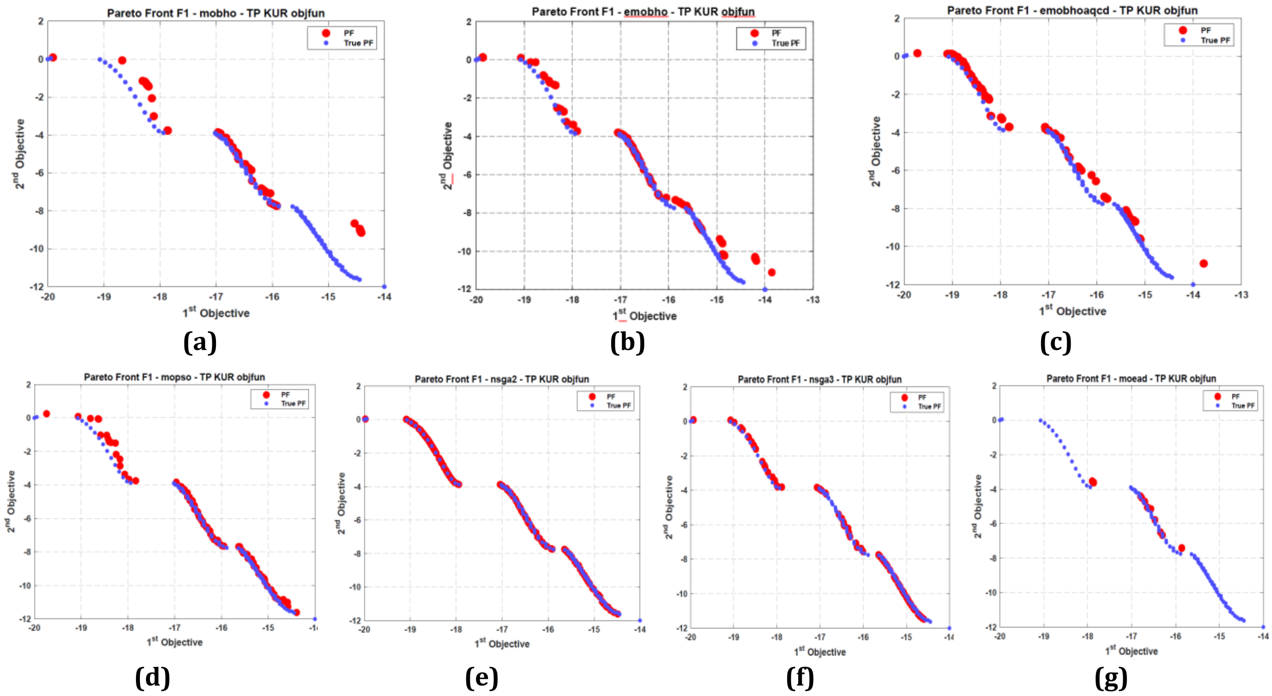

Fig.5 *Kursawe's problem comparison of the seven algorithms (a) EMOBHO; (b) MOBHO; (c) EMOBHO-AQCD; (d) MOPSO; (e) NSGA-II; (f) NSGA-III; (g) MOEA/D*

5.2.5 ZDT1 Problem

EMOBHO-AQCD has the highest Delta (0.9318) among BHO variants and better convergence than MOBHO (GD = 0.424 vs 0.677), validating the progressive improvement of the proposed mechanisms, as shown in Table 25. But, the entire family of the BHO versions shows a scalability weakness on this 30-variable problem, and the GD values are much larger than the GD (0.0025) of the MOPSO, which converts to dominance. Hypervolume (0.6585) and OS do not exhibit any significant differences among algorithms because the variability of the metrics is extremely high among versions of BHO, which makes them statistically meaningless.

Table 25 *ZDT1 performance metrics (30 variables)*

Performance Metric	Statistics	EMOBHO-AQCD	EMOBHO	MOBHO	MOPSO	NSGA-II	NSGA-III	MOEA/D
Delta	μ	0.9318	0.9857	1.0358	0.507	0.8099	0.8016	1.0739
	σ	0.0616	0.0659	0.117	0.0722	0.0411	0.028	0.0401
	σ2	0.0038	0.0043	0.0137	0.0052	0.0017	0.0008	0.0016
Delta with Inter.	μ	0.7857	0.951	1.0971	0.5216	0.6132	0.5768	1.1022
	σ	0.1846	0.1533	0.2736	0.0734	0.065	0.0473	0.0525
	σ2	0.0341	0.0235	0.0749	0.0054	0.0042	0.0022	0.0028
Generational Distance	μ	0.424	0.4409	0.6773	0.0025	0.1278	0.1307	0.0244
	σ	0.082	0.0736	0.2262	0.0005	0.0168	0.0106	0.0103
	σ2	0.0067	0.0054	0.0511	0.0	0.0003	0.0001	0.0001
Hyper Volume	μ	0.6585	0.6889	0.573	0.6352	0.6482	0.5739	0.6462
	σ	0.6627	0.5089	0.749	0.0091	0.2159	0.1685	0.1057
	σ2	0.4391	0.259	0.5611	0.0001	0.0466	0.0284	0.0112
Overall Pareto Spread	μ	0.7979	0.7965	0.6472	0.9925	0.9157	0.839	1.0425
	σ	0.7118	0.5604	0.7841	0.0101	0.304	0.2426	0.1347
	σ2	0.5067	0.314	0.6149	0.0001	0.0924	0.0589	0.0182
Uniform Dist. Euc.	μ	0.3183	0.294	0.4199	0.213	0.2328	0.2464	0.1152
	σ	0.0622	0.0874	0.1122	0.0234	0.0585	0.0679	0.0247
	σ2	0.0039	0.0076	0.0126	0.0005	0.0034	0.0046	0.0006
Uniform Dist. Avg	μ	0.3713	0.3526	0.4414	0.2587	0.28	0.3078	0.1339
	σ	0.0661	0.067	0.1294	0.0287	0.0638	0.0763	0.0234
	σ2	0.0044	0.0045	0.0167	0.0008	0.0041	0.0058	0.0005

Tables (26-27) T-test outcomes have proven that EMOBHO-AQCD is significantly better than MOBHO in GD ($p = 0.004$) and Delta ($p = 0.023$), and significantly worse than MOPSO in GD and Delta ($p < 0.01$). There is no notable difference between EMOBHO-AQCD and EMOBHO in terms of GD or HV.

Table 26 *T-test for ZDT1 (part 1)*

Metric	T-Test	emobhoaqcd emobho	emobhoaqcd mobho	emobhoaqcd mopso	emobhoaqcd nsga2	emobhoaqcd nsga3	emobhoaqcd moead	emobho mobho	emobho mopso	emobho nsga2	emobho nsga3
Delta	p	0.0752	0.0229	0.0	0.0001	0.0	0.0	0.2533	0.0	0.0	0.0
	h	0.0	1.0	1.0	1.0	1.0	1.0	0.0	1.0	1.0	1.0
Delta w/I	p	0.0429	0.008	0.0005	0.0121	0.0028	0.0001	0.1581	0.0	0.0	0.0
	h	1.0	1.0	1.0	1.0	1.0	1.0	0.0	1.0	1.0	1.0
GD	p	0.6335	0.0037	0.0	0.0	0.0	0.0	0.0056	0.0	0.0	0.0
	h	0.0	1.0	1.0	1.0	1.0	1.0	1.0	1.0	1.0	1.0
HV	p	0.9095	0.7901	0.913	0.9634	0.7003	0.9544	0.6904	0.7426	0.8185	0.5061
	h	0.0	0.0	0.0	0.0	0.0	0.0	0.0	0.0	0.0	0.0
OS	p	0.9961	0.6582	0.3987	0.6362	0.8647	0.2997	0.6303	0.2833	0.5617	0.8281
	h	0.0	0.0	0.0	0.0	0.0	0.0	0.0	0.0	0.0	0.0
UD Euc	p	0.4813	0.0221	0.0001	0.0053	0.0237	0.0	0.0118	0.0111	0.0826	0.1911
	h	0.0	1.0	1.0	1.0	1.0	1.0	1.0	1.0	0.0	0.0
UD Avg	p	0.5364	0.1444	0.0001	0.0056	0.0618	0.0	0.0697	0.0007	0.0232	0.1798
	h	0.0	0.0	1.0	1.0	0.0	1.0	0.0	1.0	1.0	0.0

Table 27 presents the remaining pairwise T-test comparisons for ZDT1.

Table 27 *T-test for ZDT1 (part 2)*

Metric	T-Test	emobho moead	mobho mopso	mobho nsga2	mobho nsga3	mobho moead	mopso nsga2	mopso nsga3	mopso moead	nsga2 nsga3	nsga2 moead	nsga3 moead
Delta	p	0.002	0.0	0.0	0.0	0.3428	0.0	0.0	0.0	0.6038	0.0	0.0
	h	1.0	1.0	1.0	1.0	0.0	1.0	1.0	1.0	0.0	1.0	1.0
Delta w/I	p	0.0086	0.0	0.0	0.0	0.9546	0.0085	0.0608	0.0	0.1701	0.0	0.0
	h	1.0	1.0	1.0	1.0	0.0	1.0	0.0	1.0	0.0	1.0	1.0
GD	p	0.0	0.0	0.0	0.0	0.0	0.0	0.0	0.0	0.648	0.0	0.0
	h	1.0	1.0	1.0	1.0	1.0	1.0	1.0	1.0	0.0	1.0	1.0
HV	p	0.7977	0.7958	0.7638	0.9972	0.7633	0.8517	0.2654	0.7485	0.4022	0.9789	0.2657
	h	0.0	0.0	0.0	0.0	0.0	0.0	0.0	0.0	0.0	0.0	0.0
OS	p	0.1938	0.1808	0.3262	0.4695	0.1336	0.4348	0.061	0.2571	0.541	0.2434	0.0324
	h	0.0	0.0	0.0	0.0	0.0	0.0	0.0	0.0	0.0	0.0	1.0
UD Euc	p	0.0	0.0	0.0002	0.0006	0.0	0.3329	0.1581	0.0	0.6372	0.0	0.0
	h	1.0	1.0	1.0	1.0	1.0	0.0	0.0	1.0	0.0	1.0	1.0
UD Avg	p	0.0	0.0004	0.0023	0.0115	0.0	0.3483	0.0729	0.0	0.3883	0.0	0.0
	h	1.0	1.0	1.0	1.0	1.0	0.0	0.0	1.0	0.0	1.0	1.0

A Wilcoxon analysis (20 paired runs) indicates that the three proposed variants have mostly non-significant differences, which confirms comparable constraints to scalability. The notable difference is observed only on GD and EMOBHO ($p = 0.0438$, $d = -0.343$, small effect), meaning that there is minimal improvement with insignificant practical value. There are no statistically significant differences between MOBHO and the comparison of the metrics. Table 28 presents the Wilcoxon signed-rank test for ZDT1.

Table 28 *Wilcoxon signed-rank test for ZDT1*

Metric	AQCD vs EMOBHO (p)	Cohen's d	Effect	Significant	AQCD vs MOBHO (p)	Cohen's d	Effect	Significant
HV	0.2043	-0.195	Small	—	0.2627	-0.091	Negligible	—
GD	0.0438	-0.343	Small	✓	0.3135	-0.608	Medium	—
Delta	0.0522	-0.505	Medium	—	0.2959	-0.418	Small	—
Delta w/I	0.7369	-0.063	Negligible	—	0.9108	-0.051	Negligible	—
OPS	0.2471	-0.190	Small	—	0.7369	-0.056	Negligible	—
UDE	0.5016	-0.209	Small	—	0.8228	-0.066	Negligible	—
UDA	0.8228	-0.126	Small	—	0.8519	+0.033	Negligible	—

The results in Figure 6 show that the BHO variants yield solutions that are remote from the actual Pareto front, whereas MOPSO yields a close correspondence. These findings suggest that EMOBHO-AQCD should be applied in low-to-moderate dimensional bi-objective problems, but not high-dimensional situations.

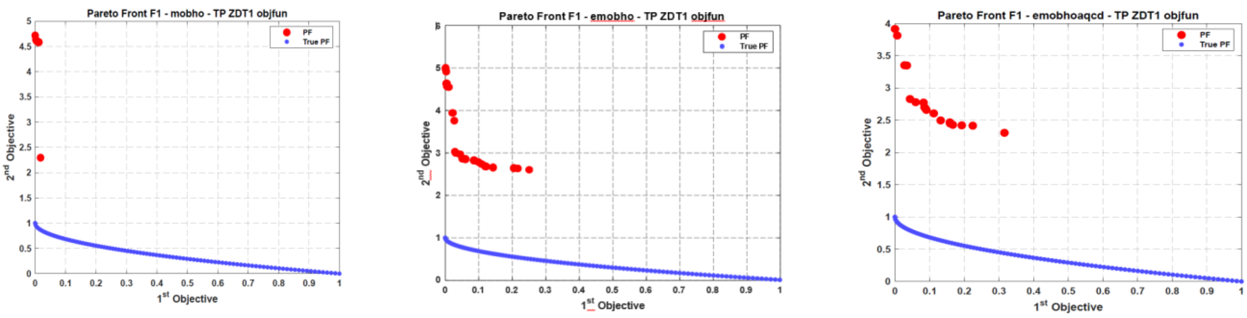

(a) **(b)** **(c)**

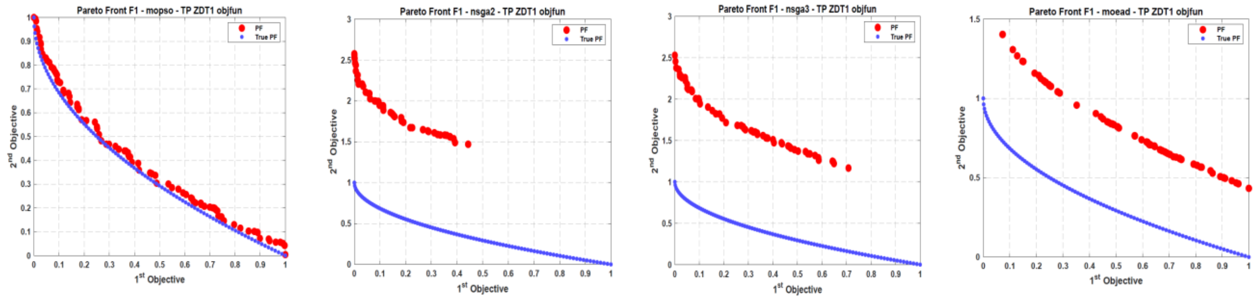

(d) **(e)** **(f)** **(g)**

Fig. 6 *ZDT1 problem comparison of the seven algorithms (a) EMOBHO; (b) MOBHO; (c) EMOBHO-AQCD; (d) MOPSO; (e) NSGA-II; (f) NSGA-III; (g) MOEA/D*

5.2.6 ZDT3 Problem

On Table 29 of ZDT3 performance metrics, EMOBHO-AQCD contains the greatest HV (1.1335) and OPS (0.804) of all algorithms, suggesting the objective range coverage is good on the discontinuous five-segment Pareto front in spite of the poor convergence (GD = 0.1878). EMOBHO-AQCD works better in HV (1.1335 vs 1.0362) and Delta (0.9937 vs 1.1038) than MOBHO, though EMOBHO remains comparable (HV = 1.0878, GD = 0.1981), which is in line with the gradual improvement of coverage behavior. Nevertheless, the convergence problems of all BHO variants are worse than MOPSO and NSGA-III (GD = 0.0008), which are close to the real front.

Table 29 *ZDT3 performance metrics*

Performance Metric	Statistics	EMOBHO-AQCD	EMOBHO	MOBHO	MOPSO	NSGA-II	NSGA-III	MOEA/D
Delta	μ	0.9937	0.9801	1.1038	0.6577	0.7367	0.8856	1.2782
	σ	0.0663	0.0418	0.1327	0.0465	0.0267	0.0549	0.0471
	σ2	0.0044	0.0017	0.0176	0.0022	0.0007	0.003	0.0022
Delta with Inter.	μ	0.9676	0.9509	1.2158	0.6397	0.6695	0.8621	1.4196
	σ	0.1238	0.0932	0.2437	0.0482	0.0354	0.0692	0.0756
	σ2	0.0153	0.0087	0.0594	0.0023	0.0013	0.0048	0.0057
Generational Distance	μ	0.1878	0.1981	0.1987	0.0008	0.0013	0.0008	0.0138
	σ	0.0347	0.0392	0.0772	0.0001	0.0003	0.0002	0.0107
	σ2	0.0012	0.0015	0.006	0.0	0.0	0.0	0.0001
Hyper Volume	μ	1.1335	1.0878	1.0362	0.7723	0.5656	0.6006	0.5469
	σ	0.9056	0.5673	0.7065	0.0082	0.1306	0.1449	0.1916
	σ2	0.8201	0.3219	0.4992	0.0001	0.0171	0.021	0.0367
Overall Pareto Spread	μ	0.804	0.7393	0.7856	0.7501	0.5319	0.5803	0.5419
	σ	0.5447	0.3417	0.4464	0.0047	0.1029	0.1289	0.1659
	σ2	0.2967	0.1168	0.1993	0.0	0.0106	0.0166	0.0275
Uniform Dist. Euc.	μ	0.1993	0.2361	0.1805	0.2001	0.1796	0.1503	0.0821
	σ	0.0856	0.125	0.0964	0.032	0.0162	0.0273	0.0203
	σ2	0.0073	0.0156	0.0093	0.001	0.0003	0.0007	0.0004
Uniform Dist. Avg	μ	0.2445	0.2658	0.1927	0.2402	0.2309	0.1731	0.0966
	σ	0.0949	0.1067	0.0983	0.0241	0.0153	0.0343	0.0201
	σ2	0.009	0.0114	0.0097	0.0006	0.0002	0.0012	0.0004

Tables 30-31 show the results of the T-test, which proves that EMOBHO-AQCD is significantly worse than classical MOEAs on GD ($p < 0.001$) and Delta ($p < 0.01$), though there is no significant difference between EMOBHO-AQCD and EMOBHO on GD ($p = 0.541$) or Delta ($p = 0.589$). The comparisons of HV and OS are not statistically conclusive because the variance is large.

Table 30 *T-test for ZDT3 (part 1)*

Metric	T-Test	emobhoaqcd emobho	emobhoaqcd mobho	emobhoaqcd mopso	emobhoaqcd nsga2	emobhoaqcd nsga3	emobhoaqcd moead	emobho mobho	emobho mopso	emobho nsga2	emobho nsga3
Delta	p	0.5885	0.0307	0.0	0.0	0.0009	0.0	0.0116	0.0	0.0	0.0004
	h	0.0	1.0	1.0	1.0	1.0	1.0	1.0	1.0	1.0	1.0
Delta w/I	p	0.7366	0.0102	0.0	0.0	0.0302	0.0	0.0048	0.0	0.0	0.0263
	h	0.0	1.0	1.0	1.0	1.0	1.0	1.0	1.0	1.0	1.0
GD	p	0.5405	0.689	0.0	0.0	0.0	0.0	0.9838	0.0	0.0	0.0
	h	0.0	0.0	1.0	1.0	1.0	1.0	0.0	1.0	1.0	1.0
HV	p	0.8938	0.7918	0.2233	0.0653	0.0827	0.0604	0.8592	0.0957	0.0109	0.017
	h	0.0	0.0	0.0	0.0	0.0	0.0	0.0	0.0	1.0	1.0
OS	p	0.7542	0.9352	0.758	0.1381	0.2224	0.1627	0.7975	0.9218	0.0827	0.1853
	h	0.0	0.0	0.0	0.0	0.0	0.0	0.0	0.0	0.0	0.0
UD Euc	p	0.4527	0.651	0.9784	0.4837	0.1017	0.0005	0.2806	0.3896	0.1736	0.0481
	h	0.0	0.0	0.0	0.0	0.0	1.0	0.0	0.0	0.0	1.0
UD Avg	p	0.643	0.2458	0.8898	0.6601	0.038	0.0001	0.1284	0.4682	0.3198	0.0175
	h	0.0	0.0	0.0	0.0	1.0	1.0	0.0	0.0	0.0	1.0

Table 31 presents the remaining pairwise T-test comparisons for ZDT3.

Table 31 *T-test for ZDT3 (part 2)*

Metric	T-Test	emobho moead	mobho mopso	mobho nsga2	mobho nsga3	mobho moead	mopso nsga2	mopso nsga3	mopso moead	nsga2 nsga3	nsga2 moead	nsga3 moead
Delta	p	0.0	0.0	0.0	0.0001	0.001	0.0002	0.0	0.0	0.0	0.0	0.0
	h	1.0	1.0	1.0	1.0	1.0	1.0	1.0	1.0	1.0	1.0	1.0
Delta w/I	p	0.0	0.0	0.0	0.0003	0.0212	0.1324	0.0	0.0	0.0	0.0	0.0
	h	1.0	1.0	1.0	1.0	1.0	0.0	1.0	1.0	1.0	1.0	1.0
GD	p	0.0	0.0	0.0	0.0	0.0	0.0001	0.9837	0.0012	0.0003	0.0017	0.0012
	h	1.0	1.0	1.0	1.0	1.0	1.0	0.0	1.0	1.0	1.0	1.0
HV	p	0.0105	0.2529	0.053	0.0722	0.0488	0.0001	0.0015	0.0016	0.5778	0.8021	0.4894
	h	1.0	0.0	0.0	0.0	1.0	1.0	1.0	1.0	0.0	0.0	0.0
OS	p	0.1176	0.8041	0.0969	0.1792	0.1229	0.0	0.0006	0.0009	0.3663	0.874	0.5704
	h	0.0	0.0	0.0	0.0	0.0	1.0	1.0	1.0	0.0	0.0	0.0
UD Euc	p	0.0012	0.5504	0.9759	0.3524	0.0054	0.0876	0.0015	0.0	0.0091	0.0	0.0
	h	1.0	0.0	0.0	0.0	1.0	0.0	1.0	1.0	1.0	1.0	1.0
UD Avg	p	0.0001	0.1553	0.2399	0.5586	0.0072	0.3198	0.0001	0.0	0.0001	0.0	0.0
	h	1.0	0.0	0.0	0.0	1.0	0.0	1.0	1.0	1.0	1.0	1.0

Table 32 shows the Wilcoxon analysis (20 paired runs) proves that EMOBHO-AQCD is much better than MOBHO on Delta ($p = 0.0304$, $d = -0.568$, medium effect), which means that it has a better spread structure. MOBHO demonstrates much improved internal spacing on UDE ($p = 0.0400$, $d = +0.554$, medium effect) and UDA ($p = 0.0251$, $d = +0.622$, medium effect), which indicates a trade-off between spacing and coverage. There is no substantial difference between EMOBHO-AQCD and EMOBHO according to Wilcoxon measures, suggesting that the two enhanced versions are equally robust on this discontinuous front.

Table 32 *Wilcoxon signed-rank test for ZDT3*

Metric	AQCD vs EMOBHO (p)	Cohen's d	Effect	Significant	AQCD vs MOBHO (p)	Cohen's d	Effect	Significant
HV	0.8228	+0.346	Small	—	1.0000	+0.503	Medium	—
GD	0.0080	-0.597	Medium	✓	0.4553	+0.061	Negligible	—
Delta	0.6813	-0.086	Negligible	—	0.0304	-0.568	Medium	✓

Metric	AQCD vs EMOBHO (p)	Cohen's d	Effect	Significant	AQCD vs MOBHO (p)	Cohen's d	Effect	Significant
Delta w/I	0.8813	-0.018	Negligible	—	0.0731	-0.528	Medium	—
OPS	0.7089	-0.062	Negligible	—	0.0731	-0.255	Small	—
UDE	0.3703	+0.097	Negligible	—	0.0400	+0.554	Medium	✓
UDA	0.2322	-0.335	Small	—	0.0251	+0.622	Medium	✓

Figure 7 indicates that EMOBHO-AQCD is demonstrating the largest segments of the BHO (with reaches of 3-4 segments), MOBHO demonstrates fewer segments with apparent concentration, and EMOBHO is concentrated in the upper part with minimal segment coverage in the lower part. Classical MOEAs have close to five segment coverage.

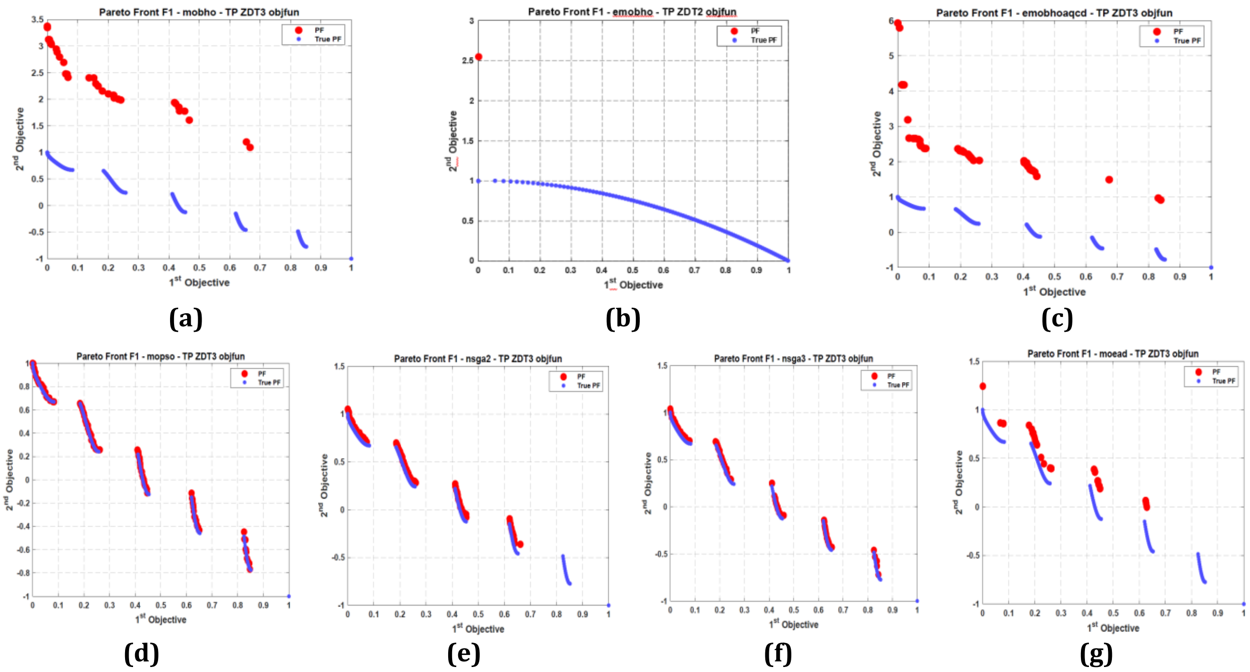

Fig.7 *ZDT3 problem comparison of the seven algorithms (a) EMOBHO; (b) MOBHO; (c) EMOBHO-AQCD; (d) MOPSO; (e) NSGA-II; (f) NSGA-III; (g) MOEA/D*

5.3 Parameter Sensitivity Analysis and Computational Cost Analysis

The results of the one-at-a-time (OAT) sensitivity analysis are shown in Table 33 with four main parameters, namely the population size (N), archive size (A), number of black holes (nBH), and the number of sectors per quarter (S), where the angle quantization factor is computed as $\alpha = \pi/(2S)$. To examine whether the performance limitations are parameter-dependent or structural, by using ZDT1 as a high-dimensional continuous benchmark, and Kursawe as a structurally challenging disconnected front. Each of the parameters was varied with the remainder of the parameters held as default parameters (N = 100, A = 100, nBH = 5, S = 4) across 10 independent runs. The most powerful effect on performance is observed with population size, where HV increases from 0.3963 ± 0.1532 (N = 25) to 0.6847 ± 0.0526 (N = 100), increasing further to 0.7497 ± 0.0332 (N = 150), with a slight decrease thereafter at 0.7402 ± 0.0624 (N = 200). The sensitivity to archive size is very low, with HV remaining constant at around 0.6847 for A = 50, 100, 150, and 200, which validates the assumption that A = 100 is adequate. The black hole count has a moderate impact: HV rises to 0.6847 ± 0.0526 (nBH = 5) compared to 0.4950 ± 0.1464 (nBH = 2), and the nBH = 5 default performs well with reduced computational expense. The range of sectors per quarter is the least sensitive, and HV is within a close range of 0.6788 and 0.7082 over the whole range of tried values, which proves the soundness of the angular discretization mechanism.

Table 33 *Parameter sensitivity analysis results*

Parameter (Default)	Value 1	Value 2	Value 3	Value 4	Value 5
Population Size N (100)	25: 0.3963 ± 0.1532	50: 0.5779 ± 0.1135	100: 0.6847 ± 0.0526	150: 0.7497 ± 0.0332	200: 0.7402 ± 0.0624
Archive Size A (100)	25: 0.6897 ± 0.0462	50: 0.6847 ± 0.0526	100: 0.6847 ± 0.0526	150: 0.6847 ± 0.0526	200: 0.6847 ± 0.0526
Black Holes nBH (5)	2: 0.4950 ± 0.1464	3: 0.6153 ± 0.1017	5: 0.6847 ± 0.0526	7: 0.7256 ± 0.0300	—
Sectors per Quarter S (4)	2: 0.7031 ± 0.0428	4: 0.6847 ± 0.0526	6: 0.7082 ± 0.0456	8: 0.6788 ± 0.0433	10: 0.6960 ± 0.0551

*nBH = 1 produced undefined (NaN) results and was excluded from the sensitivity analysis. S denotes the number of sectors per quarter, with the angle quantization factor computed as $\alpha = \pi/(2S)$. Kursawe HV = 0.000 across all parameter values and is omitted

Fig. 8 shows that there is no sharp instability in the four curves of the response of the parameters. As with the Kursawe problem, HV is always 0.0000 ± 0.0000 regardless of the parameters set, and therefore, the experimentally measured performance constraint of this disconnected Pareto front is structural rather than parameter-dependent. Such results suggest that EMOBHO-AQCD operates within a well-defined parameter space and does not require an extensive amount of fine-tuning to achieve stable performance.

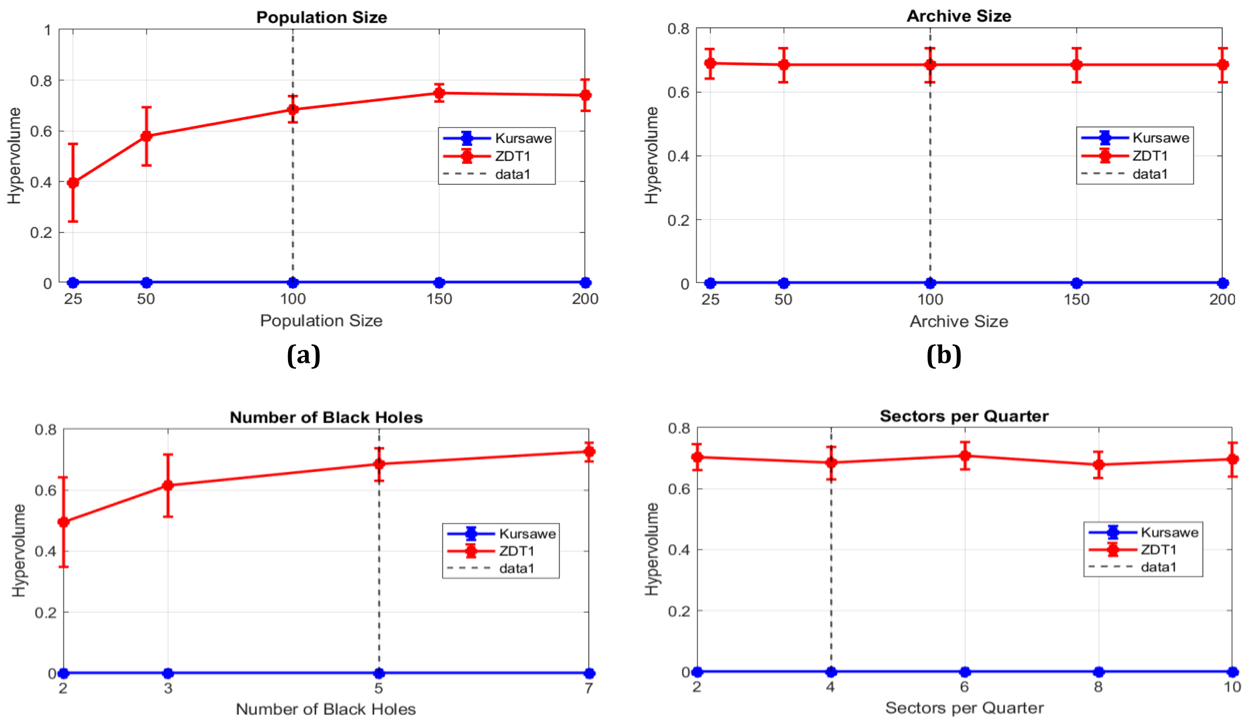

Fig. 8 *EMOBHO-AQCD parameter sensitivity plots (a) Population size; (b) Archive size; (c) Number of black holes; (d) Sectors per quarter*

As shown in Table 34, EMOBHO-AQCD has a runtime similar to that of EMOBHO and MOBHO across the six benchmark problems. The average ratio AQCD/MOBHO is 0.898, which implies that the average reduction in runtime is 10.2% compared to the baseline. The fact that energy lifecycle management does not introduce significant computational overhead is verified by the energy-enhanced variant (EMOBHO/MOBHO ≈ 0.994). EMOBHO-AQCD is noticeably faster on FON and KUR, but on SCH1, ZDT1, and ZDT3, the runtime is approximately equal to the baseline. None of the algorithms show any notable increase in runtime with the addition of energy lifecycle management, angle quantization, and crowding-distance archive control, and therefore, they do not entail any prohibitive computational cost.

Table 34 *Runtime analysis for MOBHO, EMOBHO, and EMOBHO-AQCD*

Problem	AQCD (μ ± σ, S)	EMOBHO (μ ± σ, S)	MOBHO (μ ± σ,S)
SCH1	12.58 ± 3.24	12.69 ± 2.06	12.55 ± 1.37
FON	9.75 ± 0.21	13.54 ± 0.87	13.50 ± 1.76
POL	11.91 ± 0.14	13.86 ± 1.10	12.91 ± 0.67
KUR	9.65 ± 0.10	11.33 ± 0.64	11.69 ± 0.34
ZDT1	9.54 ± 0.21	9.48 ± 0.20	9.97 ± 0.15
ZDT3	9.64 ± 0.09	9.60 ± 0.14	10.07 ± 0.24

6. Discussion

The most stable strength of EMOBHO-AQCD is manifested in the Set Coverage (SC) results. Set Coverage is a closer measure of Pareto dominance of approximation sets, which is the underlying criterion of multi-objective optimization, as opposed to proximity-based measures, like GD and HV. In SCH1, FON, and POL, EMOBHO-AQCD produces high SC1 values, which means that it resists domination by other competing algorithms. On SCH1, SC1 is almost very close to unity over all competitors, which validates that EMOBHO-AQCD can always produce non-dominated solutions that are on the same level as those produced by established MOEAs. In FON and POL, SC1 values have been found to be competitive over a variety of front geometries and are not just sensitive to simple convex cases.

In comparison to other physics-based multi-objective optimizers, EMOBHO-AQCD follows a different design philosophy from gravitational search-based methods due to its mix of adaptive black hole attraction dynamics and an organized use of an archive. In contrast to classical evolutionary algorithms, like NSGA-II and MOPSO, that depend on the selection pressure at the population level, EMOBHO-AQCD applies energy-based lifecycle control to the exploration and exploitation in the search process. This hybrid structure enables the algorithm to have a stable convergence and still maintain Pareto front coverage between benchmark geometry types, which is also consistent with the dominance robustness experienced in the Set Coverage results.

The results of this study indicate that EMOBHO-AQCD is especially efficient in preserving dominance-robust solution sets. The resulting behavior is consistent with the combined effect of angle quantization and crowding-distance archive management, which discourages clustering and favors directional coverage in the objective space. This often leads to approximation sets that are difficult for competing methods to dominate, even when the underlying Pareto front geometry is complex

One common trade-off in FON, KUR, and ZDT3 is a convergence-diversity trade-off. Where classical MOEAs like MOPSO and NSGA variants are found to converge (or have a lower GD) on some problems, EMOBHO-AQCD tends to perform better in indicators of spacing and coverage of dominance in the BHO family. As an example, Wilcoxon tests of FON indicate statistically significant differences in opposite directions in measures of hypervolume and spacing, which is a clear demonstration of this trade-off. The prioritization of distribution uniformity and directional exploration of the objective range by the algorithm in both archive and angular discretization mechanisms can be used to augment the coverage on the objective range at the cost of slowing aggressive convergence to the actual analytical front. Notably, this behavior does not imply any instability; it is simply a manifestation of a particular performance profile. A solution set that is well distributed and has wide coverage of dominance can be of more use than a tightly clustered approximation within a small region of the front.

All variants of BHO are less convergent than classical MOEAs on high-dimensional problems, including ZDT1 (30 variables). The value of GD is significantly larger than the value of MOPSO and NSGA-III, and the sensitivity analysis has shown that the value of GD does not increase proportionately to the population size. These results outline the scope of operations of EMOBHO-AQCD. The gravitational search mechanism and archive structure can also be successfully used on low-to-moderate dimensional bi-objective problems, but are less competitive as dimensionality grows and the search space becomes more difficult. This is a structural limit within the range of parameters that is tested, as opposed to a parameter-driven limit. EMOBHO-AQCD is thus best applied to continuous bi-objective problems of moderate dimensionality; the issues of dominance robustness and distribution quality are of primary interest. In large-scale or highly high-dimensional problems where a high level of convergence aggressiveness is required, classical MOEAs remain better options.

The proposed framework is limited in several ways that need to be noted despite its numerous strengths. Its current application is to bi-objective benchmark problems of moderate dimensionality, and its applicability to many-objective optimization problems remains to be explored. The present research is limited to unconstrained benchmark problems, because the initial purpose is to ensure the validation of the main mechanisms of the algorithm under controlled mathematical conditions. Future work will therefore focus on generalizing EMOBHO-

AQCD to many-objective problems, evaluating the algorithm on real-world engineering applications, including constrained optimization scenarios, and assessing its scalability to higher-dimensional decision spaces.

The comparative analysis of MOBHO, EMOBHO, and EMOBHO-AQCD is performed on a staged comparison and presents a progressive growth pattern. MOBHO gives a gravitational search foundation, and it is more variable. The performance and reduction of variance tend to be stabilized with the introduction of the energy-based lifecycle mechanism (EMOBHO) in various problems. Measurable enhancements in quality of distribution and dominance behavior on SCH1, FON, and POL are obtained using the full EMOBHO-AQCD configuration, which adds angle quantization and crowding-distance archive management. These improvements are neutral or convergence-constrained on discontinuous and high-dimensional fronts, respectively. However, the modular analysis confirms that each mechanism contributes independently to performance: stability is promoted by energy, while distribution and dominance properties are affected by AQCD. On the whole, EMOBHO-AQCD has a well-articulated performance profile. It is not expected to outperform any classical MOEAs across all metrics; it offers a dominance-oriented and diversity-sensitive alternative within the class of physics-inspired multi-objective optimizers.

7. Conclusion

In this paper, EMOBHO-AQCD, which is an energy-based multi-objective black hole optimization algorithm, was introduced that combines angle quantization and crowding-distance archive management. The algorithm was compared against four established optimizers (NSGA-II, NSGA-III, MOPSO, and MOEA/D) and two proposed baseline variants (MOBHO and EMOBHO) on six classical benchmark problems using eight complementary performance measures across ten independent runs, and also non-parametric validation was carried out using Wilcoxon signed-rank tests and Cohen's d effect size analysis. The three main findings are determined in the results of the experiment. To start with, EMOBHO-AQCD has high Pareto dominance robustness on low-to-moderate dimensional problems with SC1 values of 0.83-1.00 on SCH1, FON, and POL, and establishes consistency in resistance to domination by competitors. Second, the algorithm shows significant improvements in distribution over the MOBHO baseline, with statistically significant gains in Delta, UDE, and UDA on SCH1 and POL, with medium-to-large effect sizes. Third, a convergent-diversity trade-off is found to be systematic: the crowding-distance mechanism and angular mechanism enhance uniformity in spacing behavior and coverage behavior, and hypervolume might reduce on some problems (e.g., FON and KUR) compared to MOPSO and NSGA-II. This is indicated in statistically significant effect sizes in the opposite direction on FON (HV: $d = -1.206$, UDA: $d = -1.490$) that display a distinctively defined performance profile rather than variability. Comparative analysis of MOBHO, EMOBHO, and EMOBHO-AQCD establishes the fact that the performance went up in a progressive manner among the three variants. Management of the energy lifecycle minimizes variance in performance as well as stabilizes convergence behavior, whereas the introduction of angle quantization and control of crowding-distance archive enhances the quality of distribution and dominance properties on continuous moderate-dimensional fronts. On low-to-moderate dimensional problems, EMOBHO-AQCD is superior on both distribution and dominance measures, compared to MOBHO and EMOBHO, and on dominance measures, compared to established MOEAs. In higher-dimensional problems (ZDT1 and ZDT3), all the variants of BHO principles have obvious convergence limits compared to MOPSO and NSGA-III, and, therefore, outline the scope of operation of the presented approach. In the parameter ranges that are under analysis, these scalability constraints seem to be structure-based, not parameter-driven. EMOBHO-AQCD is therefore the most appropriate to use in low-to-moderate dimensionality bi-objective problems that are characterized by continuous or weakly discontinuous Pareto structures, where robustness in dominance and quality of distribution is a priority. It is also confirmed in the runtime analysis that the addition of energy lifecycle regulation, angle quantization, and crowding-distance archive management does not introduce prohibitive computational cost, and the mean runtime ratio is found to be 0.898 compared to that of the MOBHO with all six benchmarks. Future development will focus on hybrid decomposition-based extensions to scale to high-dimensional, adaptive energy scheduling under convergence feedback, and on testing on real-world engineering optimization problems where distributional quality and dominance robustness are important decision factors.

Acknowledgment

The authors would like to thank Universiti Tenaga Nasional (UNITEN) for providing the research facilities and computational resources used in this study.

Conflict of Interest

The authors declare that there is no conflict of interest regarding the publication of this paper.

Author Contribution

The authors confirm contributions to the paper as follows: ***study conception and design****: Zeyad Bakri and Salman Yussof;* ***data collection****: Zeyad Bakri;* ***analysis and interpretation of results****: Zeyad Bakri, Salman Yussof, Nur Fadilah Ab Aziz, and Mustafa Musa Jaber;* ***draft manuscript preparation****: Zeyad Bakri. All authors reviewed the results and approved the final version of the manuscript.*

References

[1] Deb, K., Pratap, A., Agarwal, S., & Meyarivan, T. (2002). A fast and elitist multiobjective genetic algorithm: NSGA-II. IEEE Trans. Evol. Comput., 6(2), 182–197. https://doi.org/10.1109/4235.996017

[2] Fonseca, C. M., & Fleming, P. J. (1995). An overview of evolutionary algorithms in multiobjective optimization. Evol. Comput., 3(1), 1–16. https://doi.org/10.1162/evco.1995.3.1.1

[3] Trivedi, A., Srinivasan, D., Sanyal, K., & Ghosh, A. (2016). A survey of multiobjective evolutionary algorithms based on decomposition. IEEE Trans. Evol. Comput., 21(3), 440–462. https://doi.org/10.1109/TEVC.2016.2608507

[4] Tanabe, R., & Ishibuchi, H. (2019). A review of evolutionary multimodal multiobjective optimization. IEEE Trans. Evol. Comput., 24(1), 193–200. https://doi.org/10.1109/TEVC.2019.2909744

[5] Li, K. (2024). A survey of multi-objective evolutionary algorithm based on decomposition: Past and future. IEEE Trans. Evol. Comput. https://doi.org/10.1109/TEVC.2024.3357495

[6] Deb, K., & Jain, H. (2013). An evolutionary many-objective optimization algorithm using reference-point-based nondominated sorting approach, part I: Solving problems with box constraints. IEEE Trans. Evol. Comput., 18(4), 577–601. https://doi.org/10.1109/TEVC.2013.2281535

[7] Guo, X. (2022). A survey of decomposition based evolutionary algorithms for many-objective optimization problems. IEEE Access, 10, 72825–72838. https://doi.org/10.1109/ACCESS.2022.3188549

[8] Coello Coello, C. A., Pulido, G. T., & Lechuga, M. S. (2004). Handling multiple objectives with particle swarm optimization. IEEE Trans. Evol. Comput., 8(3), 256–279. https://doi.org/10.1109/TEVC.2004.826067

[9] Gao, X., He, F., Zhang, S., Luo, J., & Fan, B. (2024). A fast nondominated sorting-based MOEA with convergence and diversity adjusted adaptively. J. Supercomput., 80(2), 1426–1463. https://doi.org/10.1007/s11227–023–05510–3

[10] Zitzler, E., Deb, K., & Thiele, L. (2000). Comparison of multiobjective evolutionary algorithms: Empirical results. Evol. Comput., 8(2), 173–195. https://doi.org/10.1162/106365600568202

[11] Daraz, A., Malik, S. A., Basit, A., Aslam, S., & Zhang, G. (2023). Modified FOPID controller for frequency regulation of a hybrid interconnected system of conventional and renewable energy sources. Fractal Fract., 7(1), 89. https://doi.org/10.3390/fractalfract7010089

[12] Hashim, F. A., Houssein, E. H., Mabrouk, M. S., Al-Atabany, W., & Mirjalili, S. (2019). Henry gas solubility optimization: A novel physics-based algorithm. Futur. Gener. Comput. Syst., 101, 646–667. https://doi.org/10.1016/j.future.2019.07.015

[13] Połap, D., & Woźniak, M. (2021). Red fox optimization algorithm. Expert Syst. Appl., 166, 114107. https://doi.org/10.1016/j.eswa.2020.114107

[14] Hatamlou, A. (2013). Black hole: A new heuristic optimization approach for data clustering. Inf. Sci., 222, 175–184. https://doi.org/10.1016/j.ins.2012.08.023

[15] Abualigah, L., Elaziz, M. A., Sumari, P., Khasawneh, A. M., Alshinwan, M., Mirjalili, S., Shehab, M., Abuaddous, H. Y., & Gandomi, A. H. (2022). Black hole algorithm: A comprehensive survey. Appl. Intell., 52(10), 11892–11915. https://doi.org/10.1007/s10489–021–02975–6

[16] Doraghinejad, M., & Nezamabadi-Pour, H. (2014). Black hole: A new operator for gravitational search algorithm. Int. J. Comput. Intell. Syst., 7(5), 809–826. https://doi.org/10.1080/18756891.2014.966990

[17] Al-Eiadeh, M. R., Qaddoura, R., & Abdallah, M. (2024). Investigating the performance of a novel modified binary black hole optimization algorithm for enhancing feature selection. Appl. Sci., 14(12), 5207. https://doi.org/10.3390/app14125207

[18] Al-Sammarraie, H. N. N., & Jawawi, D. N. (2020). Multiple black hole inspired meta-heuristic searching optimization for combinatorial testing. IEEE Access, 8, 33406–33418. https://doi.org/10.1109/ACCESS.2020.2974239

[19] Kumar, S., Jangir, P., Tejani, G. G., Premkumar, M., & Alhelou, H. H. (2021). MOPGO: A new physics-based multi-objective plasma generation optimizer for solving structural optimization problems. IEEE Access, 9, 84982–85016. https://doi.org/10.1109/ACCESS.2021.3087739

[20] Sun, B., Chang, Y., Gao, M., Li, Z., Liu, J., & Wang, J. (2025). An improved multi-objective artificial physics optimization algorithm based on R2 indicator and its application. Meas. Control, 58(4), 538–550. https://doi.org/10.1177/00202940241292086

[21] Metiaf, A., Wu, Q., & Aljeroudi, Y. (2019). Searching with direction awareness: Multi-objective genetic algorithm based on angle quantization and crowding distance MOGA-AQCD. IEEE Access, 7, 10196–10207. https://doi.org/10.1109/ACCESS.2019.2891987

[22] Zhang, Y., Hu, W., Yao, W., Li, X., & Hu, J. (2024). A multi-objective particle swarm optimization based on local ideal points. Appl. Soft Comput., 161, 111707. https://doi.org/10.1016/j.asoc.2024.111707

[23] Rashedi, E., Nezamabadi-Pour, H., & Saryazdi, S. (2009). GSA: A gravitational search algorithm. Inf. Sci., 179(13), 2232–2248. https://doi.org/10.1016/j.ins.2009.03.004

[24] Zhou, M., Cui, M., Xu, D., Zhu, S., Zhao, Z., & Abusorrah, A. (2024). Evolutionary optimization methods for high-dimensional expensive problems: A survey. IEEE/CAA J. Autom. Sin., 11(5), 1092–1105. https://doi.org/10.1109/JAS.2024.124344

[25] Wu, C., Wu, T., Fu, K., Zhu, Y., Li, Y., He, W., & Tang, S. (2017). AMOBH: Adaptive multiobjective black hole algorithm. Comput. Intell. Neurosci., 2017(1), 6153951. https://doi.org/10.1155/2017/6153951

[26] Kursawe, F. (1990). A variant of evolution strategies for vector optimization. In H.-P. Schwefel & R. Männer (Eds.), Parallel problem solving from nature (pp. 193–197). Springer. https://doi.org/10.1007/BFb0029752

[27] Schaffer, J. D. (1985). Multiple objective optimization with vector evaluated genetic algorithms. In Proceedings of the 1st International Conference on Genetic Algorithms and Their Applications (pp. 93–100). Psychology Press.

[28] Poloni, C. (1995). Hybrid GA for multi objective aerodynamic shape optimisation. In G. Winter, J. Periaux, M. Galan, & P. Cuesta (Eds.), Genetic algorithms in engineering and computer science (pp. 397–415). John Wiley & Sons.

[29] Van Veldhuizen, D. A., & Lamont, G. B. (2000). Multiobjective evolutionary algorithms: Analyzing the state-of-the-art. Evol. Comput., 8(2), 125–147. https://doi.org/10.1162/106365600568158

[30] Zitzler, E., & Thiele, L. (1999). Multiobjective evolutionary algorithms: A comparative case study and the strength Pareto approach. IEEE Trans. Evol. Comput., 3(4), 257–271. https://doi.org/10.1109/4235.797969

[31] Zhang, Q., & Li, H. (2007). MOEA/D: A multiobjective evolutionary algorithm based on decomposition. IEEE Trans. Evol. Comput., 11(6), 712–731. https://doi.org/10.1109/TEVC.2007.892759